

CHAPTER 3. AIR PATHWAY ANALYSIS

Table of Contents

3.0 AIR PATHWAY ANALYSIS	24
3.1 OVERVIEW: AVAILABILITY OF INFORMATION AND INVESTIGATIVE RATIONALE	24
3.2 SSFL AIR EMISSIONS	24
3.2.1 Rocket Engine Tests (1948 to Present).....	24
3.2.2 Evaporative Emissions of Trichloroethene and Other Toxic Organics.....	25
3.2.3 Thermal Treatment Facility (1958 to Present).....	26
3.2.4 Stripping Towers	26
3.2.5 Emission of Radionuclides	27
3.2.6 Chemical Emission Estimates.....	27
3.2.7 Summary of Emission Estimates	28
3.2.8 SSFL Air Toxic Emissions, 1990 Through 2002.....	33
3.3 AIR DISPERSION MODELING	36
3.3.1 Overview	36
3.3.2 Meteorology.....	36
3.3.3 Air Dispersion Modeling Approach.....	41
3.3.4 Modeled Concentration Fields Resulting from Air Dispersion of Chemicals Released from SSFL ...	43
3.3.4.1 <i>Concentration Fields Associated with Rocket Testing Emissions</i>	44
3.3.4.2 <i>Concentration Fields Associated with Stripping Towers and Thermal Treatment Facility Emissions</i>	45
3.3.5 SSFL Concentration Profiles from Air Dispersion Modeling of Emissions	54
3.3.5.1 <i>TCE Concentration Profiles Associated with Rocket Engine Degreasing</i>	54
3.3.5.2 <i>TCE Concentration Profiles Associated with Storage Tank Releases and Stripping Towers</i>	55
3.3.5.3 <i>Hydrazine and Derivatives Concentration Profiles Associated with Open-Pit Burning</i>	55
3.3.6 Sensitivity Studies	65

3.0 AIR PATHWAY ANALYSIS

3.1 Overview: Availability of Information and Investigative Rationale

SSFL is located within the South Coast Air Quality Management District (SCAQMD). Air pollution controls and permits at SSFL are regulated by the Ventura County Air Pollution Control District (VCAPCD). Facilities with permits regulated by VCAPCD include conventional combustion units, a coal gasification unit, the sodium heaters, the low nitrous and sulfurous oxide combustor, and the sodium burn facility. There were some non-permitted facilities (which do not require permits), such as the solid propellant area, the propellant research area, the combustion heat transfer laboratory, the engineering chemistry lab, the continuous wave laser lab, and the coca-delta fuel farm. Various SSFL activities since the commencement of operations at the facility have resulted in releases of air toxics into the atmosphere. Such emissions include both accidental releases and chronic releases—that is, releases that happened in the course of SSFL facilities' routine operations.

Except for accounts of accidental TCE releases (CH2M Hill, 1993), Rocketdyne has compiled no historical accident accounts (e.g., of tank ruptures). It also appears there has been no monitoring of offsite chemical concentrations or estimates via dispersion modeling; if such information exists, it has not been made available to the UCLA study team (Lafflam, 1989; ICF Kaiser, 1993). No air monitoring data were found for hydrazines, which is surprising considering how often hydrazines are used. Both EPA and DOE expressed concern about inadequate air sampling on site and off site, and about the lack of onsite meteorological data for most of SSFL's years of operation (EPA, 1989a; DOE, 1989, 1990). Extensive review of SSFL-related documents revealed that there are incomplete records of emissions during years of intensive rocket testing (Section 3.2, Appendix S).

Air monitoring data for chemicals of concern were not available for the offsite areas surrounding SSFL. Therefore, potential exposures associated with SSFL were assessed through analysis. In this analysis, air toxic chemicals of potential concern (COPCs) were identified (Appendix C), archived documents were reviewed and various EPA approved analysis methods were employed to estimate the significant toxic air emissions from SSFL activities (Section 3.2, Appendices S and T), and air dispersion simulations were carried out to estimate the concentration field of contaminants emitted from SSFL as illustrated in this Chapter (see also Appendix I). As expected, higher outdoor air toxic concentrations were encountered to the northeast and southwest of SSFL emissions. Outdoor air toxic concentrations decreased with distance downwind from the SSFL. The concentration field data obtained using the above analysis was combined with standard exposure analysis (Chapter 6) to assess the potential for adverse exposure levels to SSFL released air toxics (see also, Appendix T).

3.2 SSFL Air Emissions

3.2.1 Rocket Engine Tests (1948 to Present)

Rocket engine testing, or RET—shown in Figure 3-1—began at SSFL in 1948 (ATSDR, 1999). Between 1953 and 1961 over 8,000 tests on rocket engines were completed, many related to the early space missions. During the 1970s and 1980s, the site was primarily used to test engines for

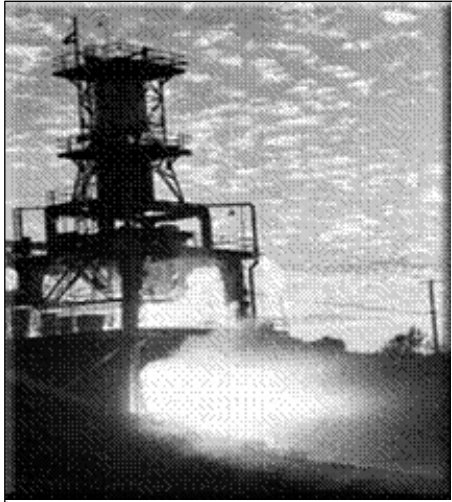


Figure 3-1. Photograph of a Rocket Engine Test.

the NASA space shuttle program, with declining numbers of tests since the 1990s. Fuels combusted at SSFL during these tests include beryllium, ethanol, hydrazine and derivatives, hydrogen, isopropyl alcohol, combinations of kerosene and liquid oxygen, as well as nitrogen tetroxide (NTO) and pentaborane (Appendix S.) Rocket test firing over the operating history of the facility routinely released products of combustion of rocket engine fuels into the atmosphere: carbon dioxide, carbon monoxide, hydrogen gas, hydrogen chloride, nitrogen gas, nitrous oxide, chlorine, metallic oxide particulates (e.g., aluminum oxide), soot, organic compounds (e.g., polyaromatic hydrocarbons, or PAHs), and volatile organic compounds (VOCs). In addition to combustion products, release of air contaminants may have resulted from activities such as accidental spills, venting after tests, cryogenic boil-off, metal plating, fuel storage and distribution, painting, and degreasing.

In the early days of RET, rocket fuels contained high levels of beryllium. Particles of beryllium were released to the air and deposited onto soil around the facility. Rockwell states that onsite beryllium-containing solids were removed from SSFL after the use of beryllium-containing fuels was discontinued (Ecology and Environment, 1991). It is noted, however, that there are monitoring data (Ogden, 1998a) indicating that beryllium may still be in soil and thus could be of an exposure concern (Ogden, 1998a; Appendix H).

3.2.2 Evaporative Emissions of Trichloroethene and Other Toxic Organics

TCE has been used at the SSFL site to flush rocket engines during degreasing (Sullivan, 1999). TCE was applied to flush rocket engines of residual fuel before and after each test. Analysis of records (CH2M Hill, 1993) suggests that typically 50 to 100 gallons of TCE were applied per engine flush. TCE was emitted to the air when this liquid evaporated.

Evaporative emissions associated with the use of TCE as a cleaning solvent in an open environment would be expected to result in significant emissions. Note that a significant percentage of the TCE produced in the United States has been used for metal degreasing, and that evaporation from degreasing is responsible for a significant percentage of the TCE released to the air. The EPA (1997, 2001a) emissions inventory program reveals that, of the total TCE solvent used in the United States, about 25% is released as fugitive emissions. Fugitive emissions associated with equipment cleaning can reach as high as 50% to 95% of the TCE used in such applications.

In addition to degreasing activities, TCE and other toxic organic air emissions (e.g., methyl chloroform, or TCA) resulted from storage tank breathing losses, emissions associated with laboratory activities, and removal from groundwater by (ST) operation (see Section 3.2.5; Rockwell International, 1994; Melvold, 1994). SSFL reportedly has had a capture system for liquid TCE spills since around 1960, but this system was reportedly unreliable (Hargis and Associates, 1985).

3.2.3 Thermal Treatment Facility (1958 to Present)

SSFL employed open-pit burning, referred to as the thermal treatment facility (TTF), to dispose of waste in Area I. The TTF was operational from 1958, destroying explosive, reactive, and ignitable wastes. Wastes sent to the TTF included ammonium perchlorate. The limited written records made available show that the TTF was periodically active for 24 to 48 hours per month every month in 1959 and 1960. Hydrocarbon disposal by open burning was prohibited by Ventura County Air Pollution Control District in 1969. However, Rocketdyne regularly applied for permission to use the burn pit with reduced volumes of waste. In 1980, the facility was permitted as a waste pile (ATSDR, 1999). Mixtures of fuels, solvents, water, and other materials were routinely burned at the burn pit (Rockwell International, 1992a; GRC, 1993; Rocketdyne, 1959–1989 [Annual Site Environmental Reports], 1959, 1960 [inter-office letters]). Among the chemicals burned at the TTF were hydrazine and hydrazine compounds, sodium pentaborane, kerosene-based fuels (e.g., RP-1, JP-4), lithium powder, nitrogen tetroxide, waste oils, TCE, solid propellants (with perchlorate as an oxidizer), chlorine trifluoride, and alcohol mixtures (Rocketdyne, 1958-1960; Rockwell International, 1992a; GRC, 1993). Disposal records indicate that burning or venting of waste materials at the TTF was conducted by the SSFL fire department, which developed and observed the disposal protocols (Rocketdyne, 1958-1960).

In 1982, the burn pit was cleaned under the Ventura County Department of Health Services' (DHS) authority (DHS, 1991). The county DHS rescinded permission for open-pit burning disposal in November 1990, after discovering logs documenting destruction of volumes of waste larger than permitted (DHS, 1991)—specifically, a slurry containing solvents and fuel. (The logs inspected by Ventura County DHS dated to April 5, May 17, and September 26, 1990; the daily limit exceeded was 5 pounds for flammable liquids.) This waste consisted of 0.6 pounds of slurry waste; 61.4 pounds of acetone, ethanol, and ethyl acetate; 27 pounds of explosives and flammable solvent mixture; and 5.14 pounds of solid explosives on the same day (April 15, 1990).

3.2.4 Stripping Towers

Carbon-adsorption/air-stripping towers are used to treat contaminated groundwater as a part of the onsite groundwater extraction and treatment program. The treatment system includes six packed tower aeration systems (at five locations) with vapor phase carbon treatment and two ultraviolet/hydrogen peroxide units. Air stripping systems were located at water supply well 9A (Delta area, Area II; 200 gallons per minute), deep well RD-1 (Happy Valley, Area I), water supply well 6 behind Alpha (Area IV; 400 gallons per minute), water supply well 9 (Bravo Area, Road I, Area I; two towers), and the Systems Test Laboratory IV (STL IV, Area II). The strippers' capacities were 40 gallons per minute except where noted (Techlaw, 1990). Permits for the operation of the strippers were limited to yearly emissions of 0.5 tons per year of reactive organics. It is noted that the VCAPCD reported that no TCE was detectable in the air stream effluent from these towers (VCAPCD, 1989). However, the UCLA study team did not receive documentation of the effectiveness of stripping treatment and the associated impact on groundwater remediation.

3.2.5 Emission of Radionuclides

Radionuclide emissions came from three sources in Area IV of SSFL: the Radioactive Material Disposal Facility (RMDF), the Hot Laboratory (HL), and the Nuclear Materials Development Facility (NMDF). The RMDF consists of several buildings where radioactive wastes are decontaminated and packaged for offsite disposal. The HL was used principally to examine and prepare radioactive waste for reprocessing. It was licensed by the Nuclear Regulatory Commission (NRC) under Special Nuclear Materials License SNM-21 and continued to work with irradiated nuclear fuels until 1988. The NMDF was constructed for research and production work involving highly radioactive fuels. It was also licensed by the NRC, but the license was rescinded after the facility was shut down in 1986 (DOE, 1989). Emissions of radioactive particulates at the three facilities were controlled by high-efficiency particulate air (HEPA) filters. There is a community concern that there may have been accidental radioactive air emissions (Appendix E).

3.2.6 Chemical Emission Estimates

To estimate emissions of toxic organic and toxic metal air emissions over the span of SSFL's operations, the audit team developed an air toxic emission inventory by:

- Reviewing documents detailing SSFL activities involving air toxics and associated emissions of specific hazardous air pollutants (HAPs).
- Estimating an air toxic emission inventory for each source of relevant HAPs at SSFL.
- Allocating total air toxic emissions by source activity as a function of time (from the late 1940s to the present).

EPA lists 188 pollutants or chemical groups as HAPs, commonly referred to as “air toxics,” that cause or are suspected of causing cancer or other serious human health effects. HAPs are emitted from thousands of sources, such as electric power utilities and industrial manufacturers, dry cleaners and gasoline service stations, and automobiles and airplanes. As shown in Figure 3-2, some of these sources are localized at individual facilities (e.g., RET), while others are ubiquitous (e.g., located at sites scattered throughout urbanized communities).

Major questions addressed in this part of the study were: What level of toxic emissions occurred over the life of this facility? What is the history of emissions at the facility? What are the most significant sources (in terms of annual release) of toxic air emissions? To guide the estimation of HAP emissions from the SSFL facility, the study team visited SSFL several times to personally observe source activity, requested available HAP air emissions information from SSFL staff, and conducted a literature review to identify and obtain other sources of SSFL emissions data. (See Appendix S for a complete emission inventory.) Information requested from SSFL included specific reports on activities identified through the literature review. A number of relevant prior studies have been identified as sources of useful information on potential emission sources and emission rates (CH2M Hill, 1993; ABB Environmental Services, Inc., 1992; Rockwell International, 1992a, 1992b; Rocketdyne, 1960).

Figure 3-2. HAP Emissions from SSFL Activities (Left) and Urban Settings (Right)



The study team identified four potentially significant sources of toxic organic and toxic heavy metal air emissions: (1) rocket engine exhaust; (2) pre- and post-degreasing of rocket engines; (3) storage tanks, STs, and other evaporative sources of toxic organic emissions; and (4) open-pit burning of waste material. The team then estimated emissions of 18 chemicals (listed in Table 3-1) by cross-referencing information about emission source types at the SSFL and the EPA HAP list (again, see Appendix S).

Table 3-1. Chemicals Analyzed for Emissions

Organics	Metals
Benzene	Arsenic
1,3-butadiene	Beryllium
Hydrazine ^a	Cadmium
TCA—methyl chloroform	Chromium
TCE—trichloroethylene	Lead
Toluene	Manganese
Xylene	Mercury
	Nickel
	Selenium
	Copper
	Zinc

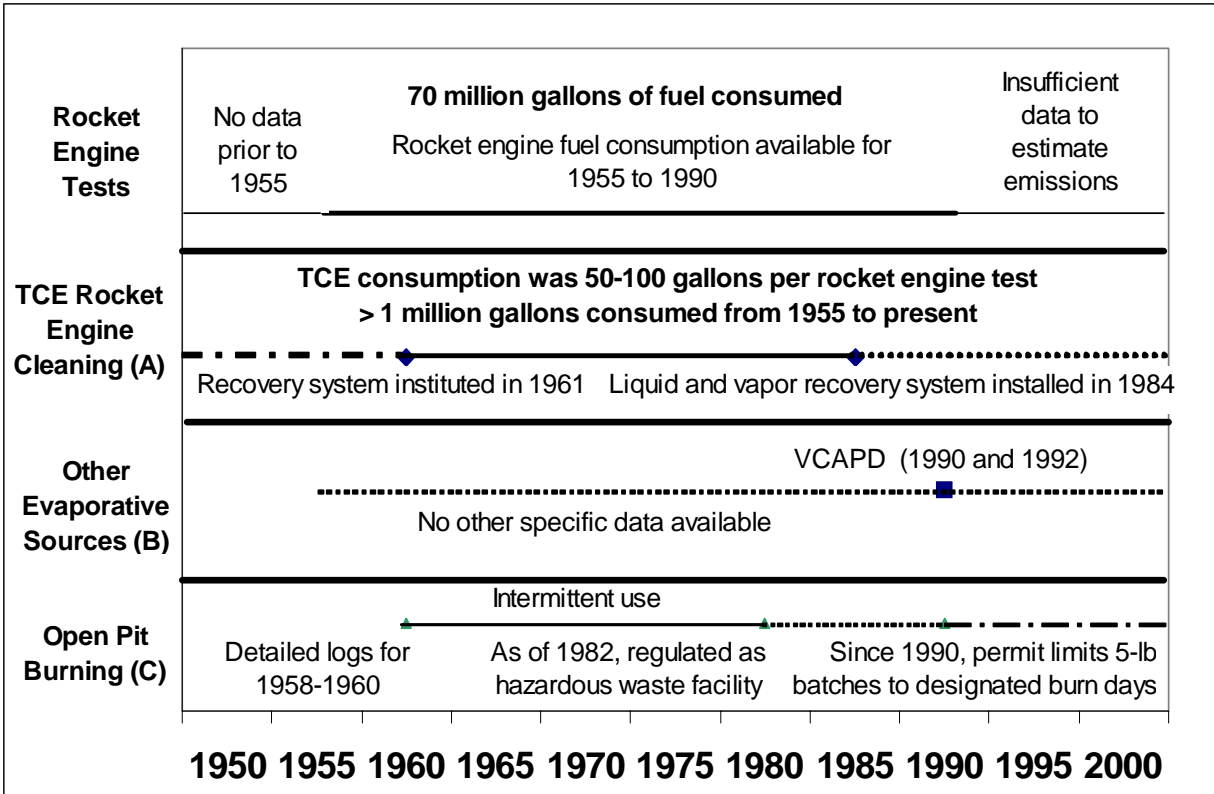
^a The hydrazine derivatives monomethyl hydrazine (MMH) and unsymmetrical dimethylhydrazine (UDMH) were also combusted during rocket engine testing in the rocket engine testing areas.

3.2.7 Summary of Emission Estimates

The study team estimated toxic organic and toxic heavy metal air emissions, from the four sources mentioned above (Section 3.2.6), for the late 1940s to the present (Appendix S). Emissions from most activities at SSFL were intermittent and have varied over time as a consequence of the changing level of activity at the facility, the introduction of control measures, and permit restrictions.

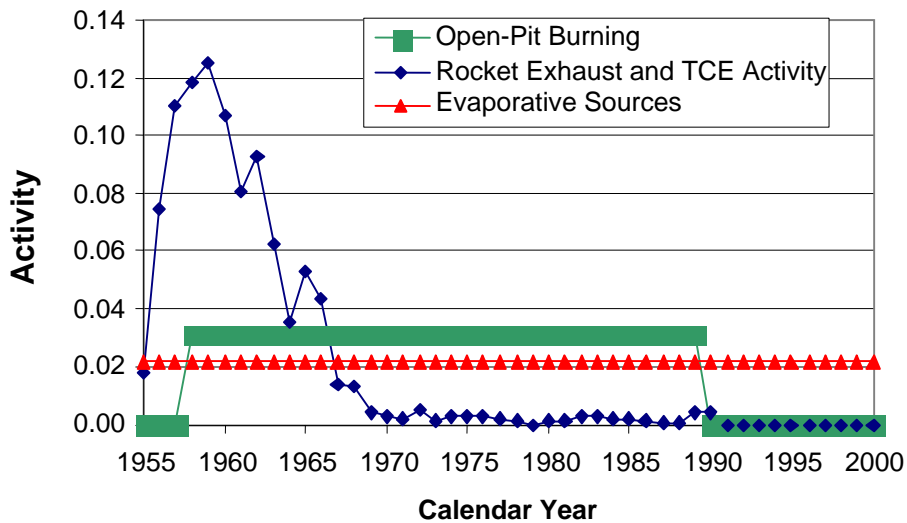
The majority (88%) of rocket exhaust emissions occurred from 1955 to 1965 (Figure 3-3). Open pit burning activity was assumed uniform from 1959 through 1989. From 1955 to 1990, cumulative toxic organic and metal emissions were about 4775 tons (including hydrazine derivatives) and 9 tons, respectively. The largest source of toxic metal emissions is rocket engine exhaust. Evaporated TCE from the cleaning of rocket engines were the largest source of toxic organic emissions to the air (Figure 3-4). Other evaporative sources (Figure 3-4) constituted the second largest source.

Figure 3-3. Timeline of Available Activity Reports for SSFL



- (A) Estimated to be the largest source of HAP air emissions.
- (B) Estimated to be the second largest source of HAP air emissions.
- (C) Not estimated to be a significant source of HAP air emissions.

Figure 3-4. History of Emissions Activity from Selected Source Types at SSFL as a Percent of Total Lifetime Activity



The available data (Appendix S) suggest that, on a weight basis, liquid kerosene was the fuel most often combusted in RET (more than 60%) from 1955 to 1990 (Table 3-2). The second most common fuel used at SSFL was liquid hydrogen (35%). Combustion of lesser amounts of isopropyl alcohol (1.4%), hydrazine derivatives (0.5%), and pentaborane fuel (0.006%) also took place. Analysis of the available fuel use data revealed that the vast majority (more than 80%) of fuel use took place before 1970; 80% of kerosene fuel use took place from 1956 through 1969, 80% of unsymmetrical dimethylhydrazine use took place between 1956 and 1965, and 96% of pentaborane use took place in 1963. The study team could not obtain fuel use data for 1948 to 1954, or for the years after 1990. Therefore, air toxic emissions resulting from fuel combustion from 1948 to 1954 and 1991 to the present could not be reliably estimated. The available documents on rocket testing at SSFL (Sullivan, 1999) did not contain fuel use data for periods before 1955 or beyond 1990. However, a review by ATSDR suggests that ethanol, kerosene, and hydrazine fuels were combusted in engines before 1955 and ethanol, kerosene, and MMH (hydrazine derivative) fuels were combusted in engines after 1990 (ATSDR, 1999; Appendix S).

Table 3-2. Reported Fuel Use at SSFL from 1955 to 1990

Fuel Name	Tons
Kerosene	173435
Liquid hydrogen	98351
Isopropyl alcohol	3765
Hydrazine and derivatives	1491
Pentaborane	16

Source: Sullivan, 1999. No data were reported for beryllium, ethanol, or any fuels from 1948 to 1954 and after 1990.

Review of SSFL documents indicates that RET at SSFL (Appendix S) has taken place at least 10 different locations; as mentioned above, there were STs in six locations and one TTF (which consisted of an open-pit burning area). Waste generated from the North American Kindleberger

Atwood Laboratory, or NAKA (in Area I, like the TTF) was sent to the TTF from 1958 to as late as 1992 (Rockwell International, 1992a). Waste generated at NAKA included HMX, RDX, nitrocellulose, nitroglycerin, and ammonium perchlorate. Other wastes sent to Area I TTF were “strong oxidizers,” hypergolic propellants (i.e., chlorine pentafluoride, tetrafluorohydrazine, and “limited quantities” of solvents and kerosene (Rockwell International, 1992). Surface water from Area I TTF can run off into the Perimeter Pond, which is part of SSFL’s reclaimed water system. It is noted that, during rainfall events, the Perimeter Pond overflows into NPDES Outfalls 001 and 002 to the south of the facility, which in turn is discharged into Bell Canyon Creek (Rockwell International, 1992a).

For air dispersion modeling purposes, the study team grouped these sources into eight RET sources (modeled as either point or area sources), six ST sources, and one TTF source. These 15 consolidated sources are summarized in Table 3-3.

Table 3-3. SSFL Emissions Sources Used in Dispersion Modeling

No.	Type	Name	SSFL Area	UTMX (m)	UTMY (m)	Point Source	Area Source
1	RET	Delta (1A, 1B, 2A, 3A, 3B)	II	343125	3788455	✓	✓
2	RET	Coca (1, 2, 3)	II	343681	3788486	✓	✓
3	RET	Bowl (PS1, VTS1, VTS2, VTS3, HTS)	I	345095	3788775	✓	✓
4	RET	Canyon	I	345383	3789055	✓	✓
5	RET	STL-IV	III	342488	3788771	✓	✓
6	RET	Bravo (1A, 1B, 2, 3)	II	343585	3789120	✓	✓
7	RET	Alfa (1, 2, 3)	II	344080	3789328	✓	✓
8	RET	APTF	I	345421	3789369	✓	✓
9	ST	Delta	II	342706	3788351	✓	
10	ST	Happy Valley	I	345509	3789109	✓	
11	ST	Alfa	I	344158	3789213	✓	
12	ST	Bravo	II	343516	3789050	✓	
13	ST	Area I Road	I	345292	3789159	✓	
14	ST	STL IV	III	342651	3788841	✓	
15	TTF	TTF	I	344318	3788324	✓	

Details of the emissions estimated from RET are summarized in Appendix S1, and estimates of TCE emission associated with engine cleaning are provided in Appendix S2. Other evaporative sources of toxic organic emissions, such as storage tanks and stripping towers, were also assessed to estimate levels of relevant air emissions (Appendix S3). Details of emissions from the TTF are provided in Appendix S4.

Table 3-4 summarizes the major cumulative air emissions of organic chemicals and metals for 1955 through 1990. TCE air releases from engine flushes are estimated to amount to about 67% of the total toxic organic emissions and about 80% of the total TCE emissions. Other evaporative losses represent about 30.5% of the total toxic organic emissions. The organics with the highest specific compound emissions in this category are TCA and TCE (46% and 54%, respectively, of the total). Emissions from RET and the TTF accounted for 2% and 0.5%, respectively, of the total emissions of toxic organics; the major compounds released were benzene, hydrazine and hydrazine derivatives, 1,3-butadiene, toluene, and xylene. The most significant source of heavy

metal emissions is kerosene rocket engine tests, with zinc, copper, and manganese constituting the largest fraction of metal emissions.

Table 3-4. Cumulative 1955–1990 Toxic Organic and Heavy Metal Emissions (Tons)

Pollutant	Kerosene Rocket Engine Tests	Hydrazine and Solid Rocket Engine Tests	TCE Engine Flushes	Other Evaporative Activities	Thermal Treatment Facility	Total
Toxic organic	95.0	2.3	3,196	1,457	25	4,775
Benzene	54.0				2.72	56.7
1,3-butadiene	18.0					18.0
Chloroform	0.04					0.04
Vinylidene chloride	0.01 (ND)					0.01 (ND)
Methylene chloride	0.01 (ND)					0.01 (ND)
Hydrazine/UDMH/MMH		2.3			20.4	22.7
Toluene	14.0				2.72	16.7
TCA				673		673
Trichloroethylene ^(a) (TCE)	0.36		3,196	784		3,980
Vinyl chloride	0.01 (ND)					0.01 (ND)
Xylene (total)	9.0					9.0
Heavy Metals	9.2	0.0				9.2
Arsenic	0.03 (ND)					0.03 (ND)
Beryllium	0.06 (ND)	0.0004				0.06 (ND)
Cadmium	0.17					0.17
Chromium (total)	0.24					0.24
Chromium (hexavalent)	0.05 (ND)					0.05 (ND)
Copper	3.1					3.1
Lead	0.03					0.03
Manganese	1.0					1.0
Mercury	0.02					0.02
Nickel	0.6					0.6
Selenium	0.03 (ND)					0.03 (ND)
Zinc	3.9					3.9

^(a) TCE emissions from the subsurface are discussed in Section 5.0.

As mentioned above, the vast majority of rocket fuel use occurred from 1955 to 1969, and TCE engine cleaning activity was similar to rocket exhaust activity. The use of TCE for cleaning of rocket engines was the largest source of toxic organic emissions to the air. The second largest source was other evaporative sources (stripping towers, degreasing activities, storage tank

breathing losses, chemical fume hoods). The largest source of toxic metal emissions was rocket engine exhaust.

The emission inventory developed in the present study provides a reasonable framework for assessing the magnitude of chemical emissions from SSFL. Such information was used to evaluate potential hot spots of exposure in the areas surrounding SSFL (Chapter 6). It is important to recognize that the analysis was based on incomplete reporting of chemical usage, site activities, accidental discharges, and emissions. For example, SSFL hydrazine and beryllium rocket engine emission measurement tests are believed to be insufficient to accurately characterize emissions and thus emissions were estimated from fuel combustion information. Air toxic emissions from fuel combustion of ethanol and isopropyl alcohol were not available and thus not included in the emission inventory. Information on accidental spills was inadequate and therefore emissions due to accidental spills of TCE, for 1955 through 1974, were estimated by data extrapolation. Annual emissions of TCA from 1955 to 1990 were assumed to be equal to that reported for 1990. No data were available from which to estimate emissions from RET before 1955 and after 1990, even though testing did occur during these periods. Finally, radioactive releases were not estimated due to lack of data; radioactive contamination was assessed based on available monitoring data.

3.2.8 SSFL Air Toxic Emissions, 1990 Through 2002

Rocketdyne provided a series of Toxic Release Inventory documents detailing estimate emissions of toxic metals and organics for 1990, 1992, and 2002, as well as parts of 1994 and 1997 (Rocketdyne, 1992, 1994a–c, 1997, 1998, 1999c, 1999d, 2003). A summary of the emission inventory data is provided in Table 3-5. Analysis of toxic metal emissions from 1990 and 2002 reveals the following:

- The annual toxic metal emissions declined over the 1990–2002 period from 9.7 to 2 pounds (about a 79% decline). Note that Rocketdyne applied lower emission factors in estimating the 1990 inventory than for the 2002 inventory, so the actual change in toxic metal emissions over the 1990–2002 period remains uncertain.
- From 1990 to 1992, total annual toxic organic emissions declined by about 10% (from 44,785 to 40,838 pounds per year); from 1990 to 2002, total annual toxic organic emissions declined by about 98.5%. This suggests a linear decline in emissions between 1990 and 2002. Four chemicals (TCA, glycol ether, methanol, and methylene chloride) accounted for 84% of the total 1990 organic emissions. TCA accounted for 75% and 62% of the air toxic organic inventory for 1990 and 1992, respectively, while there were no reported emissions in 2002. Glycol ether and methanol emissions for 1990 were reported as 1184 and 1578 pounds, respectively, with no emissions reported for 1992 and 2002. Methylene chloride emissions were 1732 and 1072 pounds for 1990 and 1992, respectively, with no emissions reported for 2002.
- Similarly, hydrogen fluoride (an inorganic species) emissions were reported in 1990 and 1992 but not in 2002. It is noted that cyclohexane was not emitted in 1990 or 1992, but was emitted in 2002. The reasons for the unexpected presence of cyclohexane in the 2002 inventory and the absence of hydrogen fluoride and methylene chloride emissions from the 2002 inventory have not been provided to the UCLA team.

The partial inventory data for 1994–1997 revealed that 1994 was the year in which TCE usage as a degreaser in RET was reportedly terminated. In the 1997 inventory, also partial, ammonia was the largest reported source of toxic inorganic and organic emissions (99.6%). Benzene and formaldehyde were not emitted in 1997, though emissions were reported for these two compounds in 1990 and 1992. It is also noted that the toxic emission inventory data reported for the 1990–2002 period are incomplete, and the reliability of the data is of concern given apparent inconsistencies that are not addressed in the Rocketdyne inventory documents.

Table 3-5. SSFL Air Toxics Emission Inventory from 1990 to the Present

Chemical	Emissions (lb/yr)													
	Total 1990	Other 1990	RET 1990	Total 1992	Other 1992	RET 1992	1994	Add'l 1997	Total 2002	Other 2002	Alfa 2002	Bravo 2002	APTF 2002	
1,2,4-Trimethylbenzene										10				
1,3-butadiene	172		172	76		76		0	15	11	3.6400	0.63400	0.0057900	
Acetaldehyde				36	1	34		2	1		1.2200	0.22100	0.0019400	
Acetone				1030	1030				0					
Acrolein								0		1				
Ammonia				549	549			12074						
Benzene	568	49	519	141	92	49		0	65	52	11.0000	1.90000	0.0175000	
Carbon tetrachloride	305	305		0	0				2	2				
Chloroform	58	58		1		1			0		0.0081	0.00140	0.0000129	
CFC-113									0					
Cyclohexane				0	0			4	207	207				
Ethylene dichloride	526	526												
Formaldehyde	309	2	307	72	36	36		1	41	33	6.3800	1.10000	0.0101000	
Gasoline vapors	228	228												
Glycol ethers	1184	1184		0	0			5	0					
Hydrogen fluoride	29	29		35	35				0					
Isopropyl alcohol				3851	3851				349	349				
Methanol	1578	1578						5						
Methylene chloride	1732	1732		1072	1072				0		0.0025	0.00040	0.0000040	
PAH				213	213			0	0					
Phenol	1051		1051	91	91				21		17.7000	3.08000	0.0282000	
sec-butryl alcohol				536	536				0	0				
TCA	37399	37399		25467	25467				0					
TCE	4305	1497	2808	7756	7756		0		0		0.0735	0.01280	0.0001170	
Toluene	261	129	132	72	59	13		13	3		2.7800	0.48600	0.0044200	
Xylene	159	70	89	50	50			15	2		1.8600	0.32300	0.0029600	
Vinylidene chloride				0	0	0			0		0.0024	0.00042	0.0000038	
Vinyl chloride				0	0				0		0.0025	0.00043	0.0000039	
Total	49864	44785	5078	41047	40838	210	0	12117	719	666	44.6690	7.75944	0.0710516	
Arsenic			1.7E-02						4.E-03		0.0040	0.00004	0.0000063	
Beryllium			3.2E-02						7.E-03		0.0066	0.00042	0.0000106	
Cadmium			1.1E-01						3.E-02		0.0342	0.00005	0.0000544	
Chromium			1.5E-01						1.E-03	5.1E-04	0.0004	0.00004	0.0000007	
Copper			1.7E+00						6.E-01		0.5990	0.00004	0.0009520	
Lead			2.3E-01						6.E-01		0.5990	0.00042	0.0009520	
Manganese			6.2E-01						2.E-01		0.1920	0.00085	0.0003040	
Mercury			2.5E-02						3.E-03		0.0034	0.00003	0.0000054	
Nickel			3.940						1.E-01		0.1220	0.00255	0.0001940	
Selenium			3.2E-02						7.E-03		0.0066	0.00042	0.0000106	
Zinc			2.4E+00						8.E-01		0.7630	0.00255	0.0012100	
Chromium VI			0.402						8.E-04		0.0008	0.00000	0.0000013	
Total			9.749						2	0.0005	2.3311	0.00742	0.0175000	
	24-Feb-94			8-Jun-94			22-Jul-94			1-Feb-98				
	31-Jul-97		From Nov. 1996 to Apr. '97					13-Oct-92		Less than ABB estimates				
	4-Sep-03													

3.3 Air Dispersion Modeling

3.3.1 Overview

Spatial patterns of contaminant concentrations resulting from SSFL emissions were assessed by numerical air dispersion modeling. The first objective was to decide whether available meteorological data were representative of meteorology during the years SSFL has been operating (1948 to the present). The second objective was to model air dispersion of emissions from RET, cleaning solvents, stripping towers (STs), and open-pit burning at the TTF. Estimated concentration patterns were then used, along with various exposure scenarios, to identify areas of potential exposure concern surrounding SSFL. Review of the available climatological data suggests that the available meteorological data from 1994 to 1997 are reasonably representative of the period of historical operations at SSFL (Appendix I).

3.3.2 Meteorology

The use of a few years of meteorological data for to assess dispersion modeling relevant for longer time periods is a reasonable approach, provided that the few meteorological years selected are consistent with the longer climatological data history. In order to assess the suitability of the four years (1994–1997) of available on-site meteorological data for representing the historical time period, precipitation and temperature data in the four available meteorological years were compared with climatological precipitation and temperature data during the period of 1948 through 2002. The precipitation assessment is briefly described below and the temperature assessment is discussed in Appendix I. The study team also sought to assess the diurnal variations of on-site winds at SSFL. Understanding the wind flow directions is relevant as emissions follow the wind direction pattern.

The nearest meteorological station to SSFL with long-term annual precipitation totals is in Canoga Park, California at a distance of only 15 kilometers (9.3 miles) southeast of SSFL. The proximity of the above station to SSFL provides a reasonable justification for considering precipitation data at Canoga Park to be representative of the yearly precipitation pattern at SSFL. At Canoga Park, the annual average rainfall of 16.2 inches during 1949-2002 (Figure 3-5) is 10% less than the 17.0 inches for the 1994-1997 period. The standard deviation of the annual average rainfall of 9.1 inches for 1949-2002 is 13% higher than for the 1994-1997 period. Given that the annual and standard deviation precipitation statistics for the 1948-2002 period and the meteorological data period (1994-1997) deviate by at most 13%, the SSFL on-site data for 1994-1997 seem appropriate for representing the longer air quality study period.

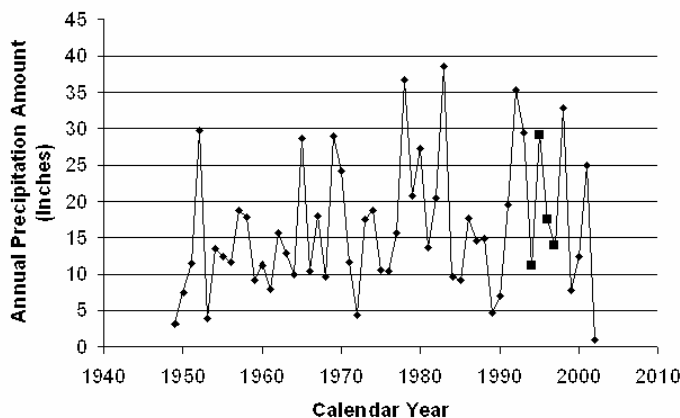


Figure 3-5. Annual Precipitation Totals from 1948 to 2002 at Canoga Park, California

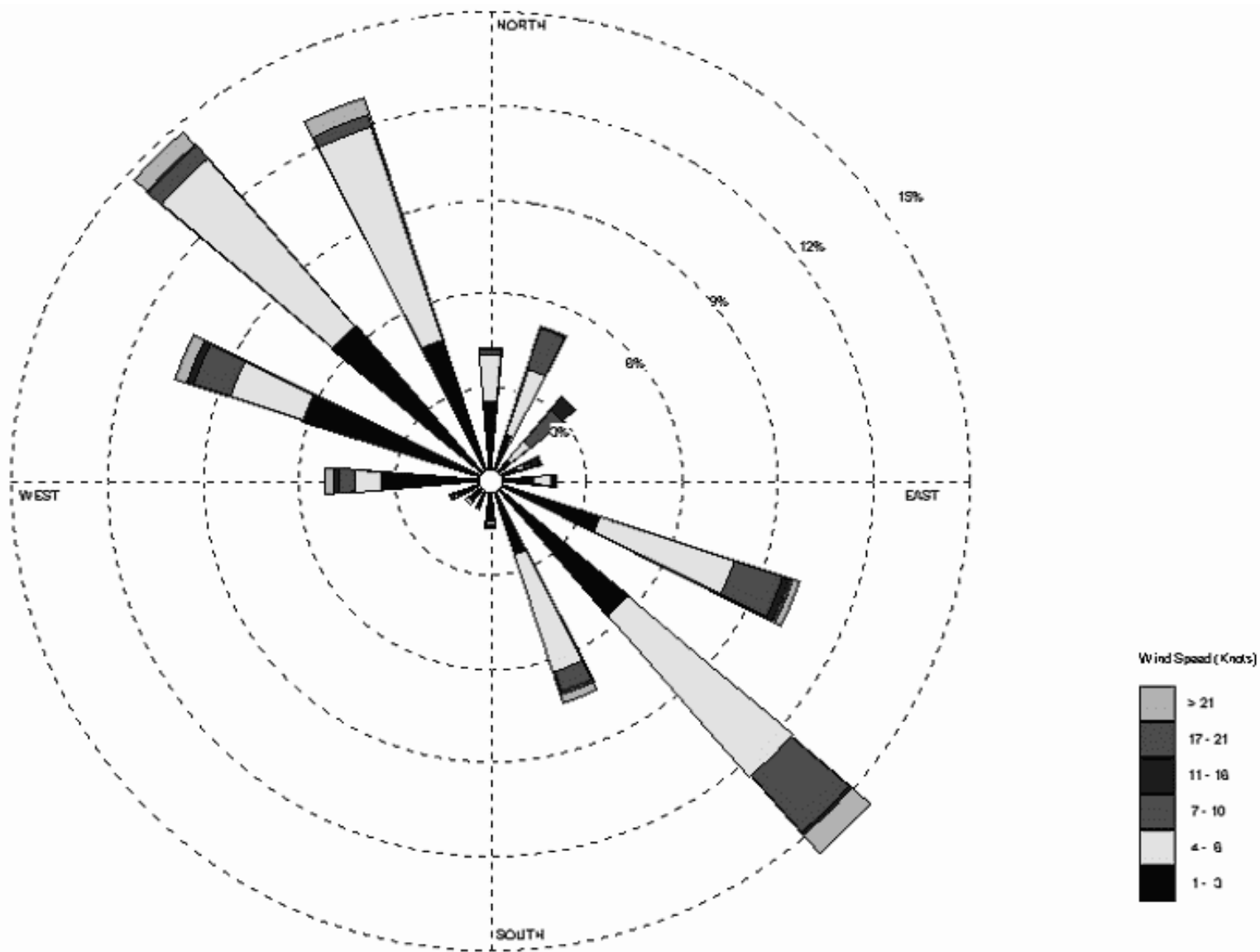
The frequency of wind speeds and wind directions^{3.1} measured in SSFL Area IV (Figure 2-2) from 1994 to 1997 by 16 compass directions by time of day are illustrated using three wind rose plots. A wind rose diagram shows the frequency of measured wind speeds and wind direction. A wind rose plot contains a center circle from which 16 thick lines emanate. The length of each line corresponds to the frequency of measured winds in that compass direction. The average wind pattern across all hours of the day from January 1994 through December 1997 is shown in Figure 3-6. Most winds (85%) flow from the northwest to the southeast and in reverse. This is nearly the same wind pattern followed from 7 a.m. to 8 p.m. (0700 to 2000 PST) (Figure 3-7). Wind flow from the southwest and northeast quadrants were significantly less at 3% and 12% of the time, respectively. Therefore, using this SSFL wind data continuous and daytime into late evening air emissions should result in similar surrounding air impact patterns. According to the wind direction pattern, the highest impacts will be southeast and northwest of SSFL emission sources. Figure 3-8 shows a different wind pattern for the time period 11 a.m. to 8 p.m. (1100 PST to 2000 PST) from January 1994 through December 1997. Winds are mostly from the northwest. Therefore, SSFL sources of air emissions emitted only or predominately in this time period should result in surrounding air impacts highest southeast of SSFL emissions. This time period from 11 a.m. to 8 p.m. is when most emissions from SSFL RETs probably occurred (S. Laflam, personal communication, 1994). These facts suggest SSFL RETs and TCE flushes are likely to have resulted in the highest surrounding air impacts southeast of the SSFL. These wind patterns are consistent with main flow directions in the region and local terrain.

Like all local wind data, the Area IV wind data were most accurate for the local area of the measurement. Study team members personally observed that SSFL Area IV wind directions were consistent with those in SSFL Areas II and III but not with Area I. To better understand the inconsistent wind directions in Area I compared with Areas II, III and IV the following is noted. SSFL collected wind data in Area I are rotated about 22 degrees counterclockwise compared with Area IV wind data. The 22 degree wind rotation in Area I is consistent with a downward directional slope of the dominant ridge in that area. Therefore, this wind rotation in Area I is likely present only south of this dominant local terrain ridge^{3.2}. This variation in flow pattern often occurs in light winds when terrain effects dominate and cause upslope and downslope flows. Analysis of the light winds frequency revealed that surface winds were less than 2 knots 25% of the time and less than 4 knots 45% of the time. Therefore, upslope and downslope weather patterns may have occurred at least 25% and possibly as often as 45% of the time. This bidirectional wind flow behavior was not incorporated in the model simulations, since wind data for Area I were not available for the same periods as the Area IV data. A complex computer wind field model that includes the detailed site topography could in principle be used to evaluate this bidirectional wind flow. Such an endeavor was beyond the scope of this study, for which the present approach is believed to be sufficiently conservative to identify the locations of potential exposure concern.

^{3.1} Precise Environmental Consultants reviewed the preprocessed meteorological data and noted a systematic scaling error (Suder, 1999). The data were corrected and compared to other meteorological data collected in Area I (see Figure 2-2) for October 1998 through April 1999. The corrected winds from Area IV were found to be consistent with the winds from Area I. These corrected wind data from Area IV were used in the present modeling work.

^{3.2} Emission sources south of this ridge include the TTF and five RET areas (the Bowl, Canyon, APTF, Coca, and Delta areas).

Figure 3-6. Wind Rose Plot of Surface Wind Data from SSFL Area IV: All Hours, Years 1994–1997



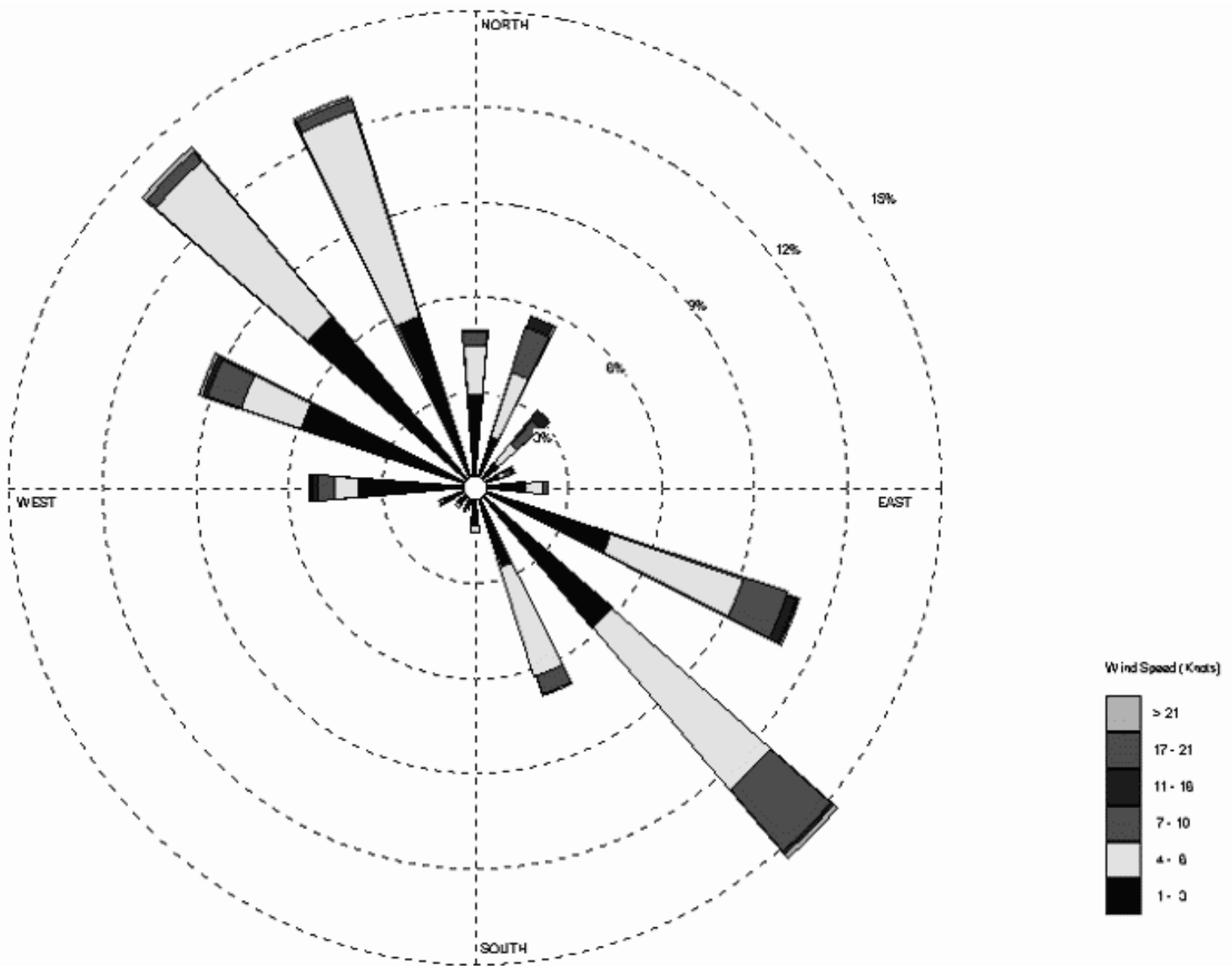


Figure 3-7. Wind Rose Plot of Surface Wind Data from SSFL Area IV: 0700–2000 PST, Years 1994–1997

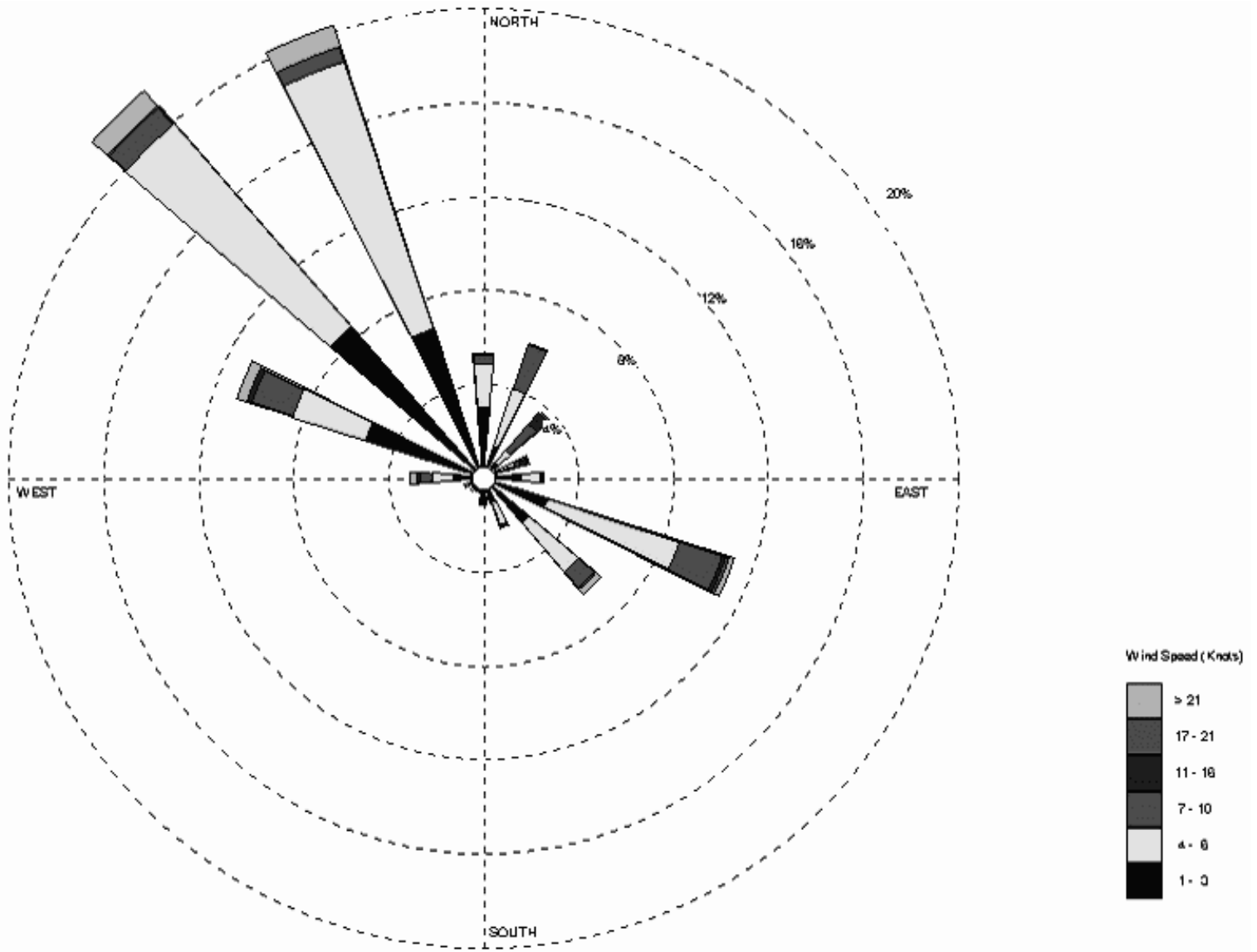


Figure 3-8. Wind Rose Plot of Surface Wind Data from SSFL Area IV: 1100–2000 PST, Years 1994–1997

3.3.3 Air Dispersion Modeling Approach

Dispersion of SSFL emissions into the atmosphere and the resulting outdoor concentrations in various communities surrounding the SSFL were estimated using the CALPUFF air quality model (EPA, 1995c, 1998, 2001). CALPUFF is an EPA approved model that is capable of predicting airborne concentrations of multiple species simultaneously. The CALPUFF model requires input of receptor coordinates at which to predict ambient air concentrations. In the CALPUFF model, receptors can be specified in an organized polar or rectangular grid or as discrete receptor locations. Meteorological data are input as hourly averages. Model input data for CALPUFF include source characteristics, meteorological data, and topographical data.

Meteorological data for the period 1994-1997 from SSFL Area IV were prepared into the single height data format for use in CALPUFF. This data format is identical to that used in the EPA ISC steady state Gaussian model (EPA, 1995). CALPUFF predicted concentrations were obtained at locations spaced 1000-meters (about 0.6 miles) apart extending to a distance of 50 km (~ 31 miles) radially from SSFL. This grid enabled estimates of airborne concentrations within various communities (Fig. 2-9) within 31 miles of SSFL. CALPUFF simulations were also carried out with locations spaced 100 meters (~ 0.06 miles) apart to provide refined coverage near the SSFL property. The terrain elevations of the various receptor locations are provided in Appendix I.

CALPUFF simulations were carried out for 39 different emission scenarios (Appendix I, Table I-8):

- Thirty-two (32) simulations were run to predicted airborne concentration patterns resulting from RETs. Four simulations were carried out for each of the eight RET locations. The four simulations at each location consisted of two simulations of RET emissions and another two simulations of the TCE emissions that resulted from degreasing the rocket engine equipment. The two simulations of RETs and TCE degreasing emissions used a constant and a best-estimate of the daily variation in emissions. The best-estimate was derived from anecdotal evidence and safety issues, which suggested that RET occurred almost only during daylight and dusk. It is believed that for safety reasons engines were tested on the same day they were prepared for testing. This suggested that, when averaged over all days in the historic period, the number of engine tests increased from morning to dusk. The study team used this “best estimate” in the modeling study for the RET emissions. As a sensitivity study, the ambient impact of RET emissions was also examined assuming testing took place uniformly throughout the day and night. It is noted that the best-estimate and uniform emission scenarios represent two extremes of emission alternatives.
- Six simulations were conducted for the STs (one for each ST source). Organic emissions from air stripping were assumed constant and diurnally invariant. This is consistent with the assumption of continuous use of the equipment.
- One simulation was made for the TTF source. In this simulation it was assumed that open pit burning occurred only during the daytime (due to safety reasons) and at a constant uniform rate.

The diurnal profiles used to model emissions from RET, ST, and TTF sources are give in Table I-8 (Appendix I). Detailed building geometry data over the lifetime of the SSFL facility were not available, so it was not feasible to include downwash in the model simulations. it was not possible to include downwash accurately in the RET simulations. Therefore, this study treated dispersion simulations of RET emissions conservatively without significant buoyancy.

Additional simulations were made to evaluate the sensitivity of predicted concentrations to atmospheric degradation and rain scavenging. Both of the above processes lead to reduced airborne concentrations of the emitted air toxics. It is noted that winds were less than 2 knots about 25% of the time. Therefore, it was possible for emitted air toxics to be transported a distance of less than 2 miles (about 3 kilometers) in an hour for only about 25% of the time. This implies that since the atmospheric chemistry half-lives of the COCs (except for the secondary species 1,3-butadiene) is above 1-hour, atmospheric degradation was not a relevant factor in the near field (except for 1,3-butadiene). Removal of air toxics from the atmosphere by rain scavenging is an episodic process. However, since rainfall occurred less than 2.1% of the total annual hours, rain scavenging would have a negligible impact on the long-term average atmospheric concentrations of air toxics emitted at SSFL. Therefore, the team omitted the effect of rain on reducing airborne concentrations.

All CALPUFF simulations were accomplished using a source specific “unit emission rate”^{3.2} of 1 milligram a second. Specific air toxic concentration fields were estimated from this information as follows. For each specific air toxic, the CALPUFF results by source location were multiplied by the specific air toxic emission rate (in milligrams a second) for that source. Added together were the specific air toxic airborne concentrations predicted from the individual sources to calculate the air toxic combined effect from all SSFL emission locations. CALPUFF output was in the form of outdoor concentrations for short (1-hour) periods and four-year averages, for the various receptor locations, with post-processing performed to obtain get long-term (annual or multi-annual) averages.

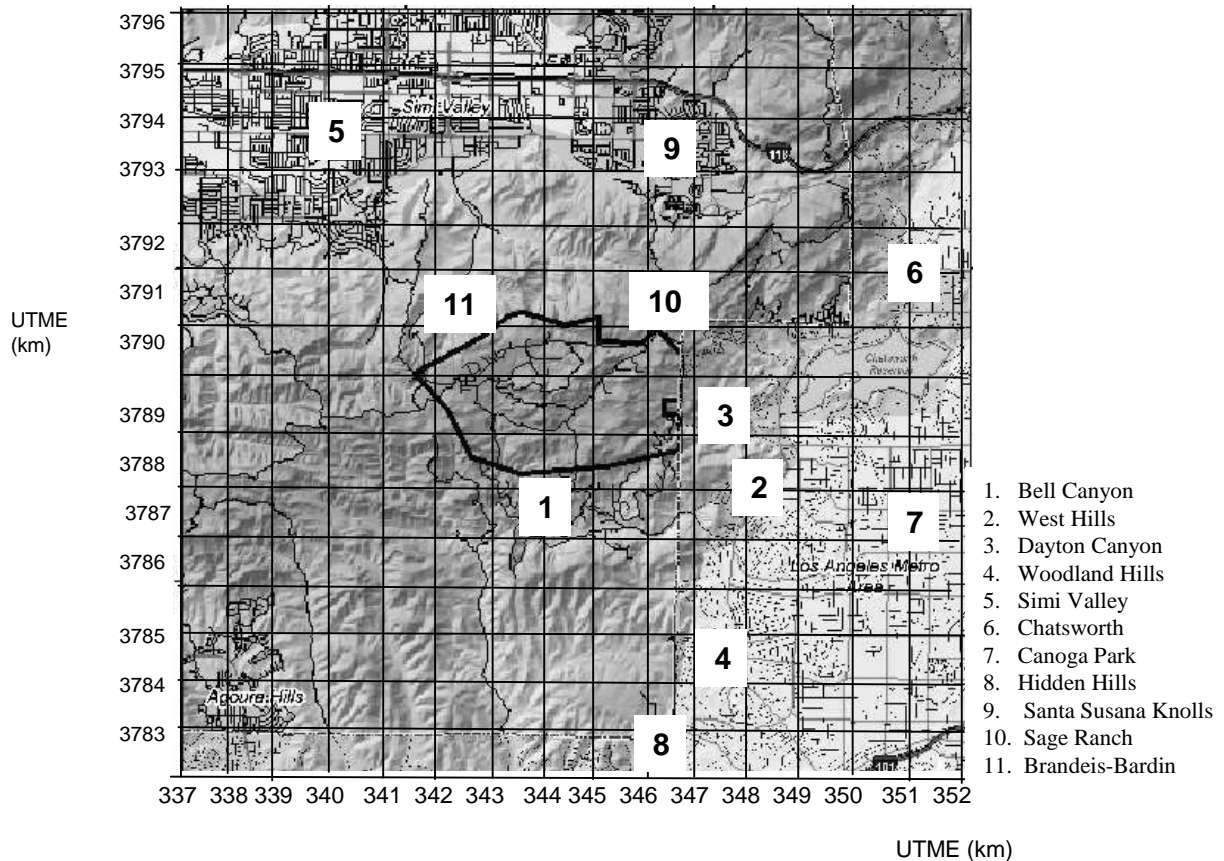
The concentration fields obtained from the various simulations served to identify locations of peak predicted concentrations at or beyond the SSFL property boundary. For each of these peak concentrations, the corresponding meteorological date (month, day, year) and time (hour of day) were identified along with the emission source that represented the highest contributing to each of the peak concentration. In order to assess the upper limit of the emission impacts, the highest concentration location on the SSFL property boundary was also identified. The average concentration by hour-of-day averaged over the four-years of hourly predicted concentrations was calculated at this location. A review of these hour-of-day averages identified the time of day when exposure at such location was expected to be highest and lowest. Finally, to assess how air toxic concentration, on any single day during the four years modeled, might vary from the AAC, the highest daily average concentration (DAC) was calculated at the SSFL property boundary to provide a frequency distribution of DACs.

^{3.2} For example, to estimate concentrations for an emission rate of 1 ton per year, the modeled concentration at 1 gram per second would need to be multiplied by 907,185 grams and divided by 31,536,000 seconds, which in this case would be about 3% of the concentration at 1 gram per second.

3.3.4 Modeled Concentration Fields Resulting from Air Dispersion of Chemicals Released from SSFL

Dispersion modeling results are summarized in contour plots overlaid on a map of the area surrounding SSFL (Figure 3-9). These contour plots illustrate the historical ambient air concentration pattern predicted by CALPUFF to have occurred around the SSFL facility from each source activity. As a reference, the figure shows the locations of a number of selected communities on the area map with the corresponding receptor grid coordinates. Each of the concentration fields plotted in Figures 3-10 to 3-15 covers an area of approximately 15 by 15 kilometers, centered over SSFL. (The boundary of the SSFL is outlined in white at the center of each plot.) To visually reflect this predicted behavior, the CALPUFF predictions are plotted using log normal contours that change in multiples of 10 (e.g., $10^{-3} \mu\text{g}/\text{m}^3$, $10^{-2} \mu\text{g}/\text{m}^3$, $10^{-1} \mu\text{g}/\text{m}^3$, $1 \mu\text{g}/\text{m}^3$, $10 \mu\text{g}/\text{m}^3$). In other words, contours are plotted at intervals of 0.2 orders of magnitude, which means that every fifth contour reflects a factor-of-10 change in concentration.

Figure 3-9. Receptor Coordinates of Communities



3.3.4.1 Concentration Fields Associated with Rocket Testing Emissions

Figure 3-10 depicts the AAC pattern for all RET point sources using the best-estimate diurnal emissions profile (Section 3.3.3). The pattern shows the highest concentrations within the boundaries of the SSFL and extending predominantly southeast toward the city of Canoga Park. A secondary lobe of high concentrations extends northwest toward Simi Valley. These results are consistent with the surface wind climatology for the SSFL during daylight hours.

The AAC pattern for all RET point sources using the uniform diurnal emissions profile is shown in Figure 3-11. This pattern demonstrates the sensitivity of predicted concentrations to the diurnal emissions profile used. The general pattern is similar to that predicted using the best-estimate diurnal profile, but the highest concentrations are more uniformly distributed to the southeast and northwest. In addition, secondary maxima are seen to the west-southwest and northeast. These results are consistent with the SSFL surface wind climatology for all hours.

Figure 3-12 shows the AAC pattern for all RET area sources using the best-estimate diurnal emissions profile. This pattern represents the potential impact from emissions associated with solvent (i.e., TCE) use near the RET stands. The pattern is similar to that for RET point sources (Figure 3-11), but concentrations are generally higher.

The AAC pattern for all RET area sources, using the uniform diurnal emissions profile, is shown in Figure 3-13. This pattern demonstrates the diurnal meteorological sensitivity of the predicted concentrations, assuming no diurnal variation in emissions. It also represents the potential impact from emissions associated with solvent use near the RET stands. As with the RET area source simulations with best-estimate diurnal emissions, the concentrations are generally higher than for the corresponding point source cases. However, secondary concentration maxima, as seen to the west-southwest and northeast in the corresponding point source case, are not evident.

Simulations for the best estimate diurnal emission profile from RET sources (Appendix I) demonstrated that the locations of the peak hourly concentrations are along the northeast and eastern edges of the SSFL property boundary. At the SSFL boundary line, the scenario of daily increasing emission correspondingly yielded AACs that increase during the day from 0600 to 1900 PST. The peak predicted annual average concentration was about six times greater than the AAC and occurred at 1900 PST. Note that emissions from the APTF RET stand were identified as contributing the most to the peak hourly concentration (PHC) at the SSFL property boundary.

Figure 3-14 shows PHC contours from a single RET point source (the APTF) for the best-estimate diurnal emissions profile. These concentrations are the maximum hourly concentrations for each receptor during the four years modeled and are approximately three orders of magnitude higher than for the AACs. The pattern is less defined than for the AACs, with higher concentrations in all directions. The highest concentrations outside SSFL are north of Canoga Park, toward the Chatsworth Reservoir. This pattern is likely a result of shifting wind directions when vertical mixing decreases and emissions are highest: from 1600 to 2000 PST. February 4, 1995, was identified as having the highest PHC of all days in the four years modeled. This worst-case scenario was assessed by carrying out a simulation for the above date, for a single rocket test, from 1800 to 1900 PST (winds were mostly from the West). The simulation results (Figure

3-15) indicate a concentration decline downwind of the SSFL property boundary. The downwind PHC decreases rapidly in the first 3.7 kilometers, where the PHC would be less than 10% of that at the property boundary. Beyond 3.7 kilometers, the decreases in PHC become uniform; the PHC at 31.1 kilometers is only 1% of that at the property boundary.

3.3.4.2 Concentration Fields Associated with Stripping Towers and Thermal Treatment Facility Emissions

The AAC pattern for all ST point source emissions, using the best-estimate uniform diurnal emissions profile, is shown in Figure 3-16. The pattern is similar to that obtained by modeling the RET point sources with the uniform diurnal emission profile. The AAC pattern for all TTF sources using the best-estimate (daylight only) diurnal emissions profile (Figure 3-17) is similar to that for the RET point sources using the best-estimate diurnal profile. However, it is centered over the TTF, and the maxima to the northwest and southeast are more balanced. This behavior is expected, since winds at SSFL tend to increase in strength from the northwest later in the day.

Figure 3-10. Average Concentration Pattern for all RET Point Sources Using the Best-Estimate Diurnal Emissions Profile



Figure 3-11. Average Concentration Pattern for all RET Point Sources Using the Uniform Diurnal Emissions Profile



Figure 3-12. Average Concentration Pattern for all RET Area Sources Using the Best-Estimate Diurnal Emissions Profile



Figure 3-13. Average Concentration Pattern for all RET Area Sources Using the Uniform Diurnal Emissions Profile



Figure 3-14. Contours of Locations of Highest Concentrations for the APTF Point Source Using the Best-Estimate Diurnal Emissions Profile

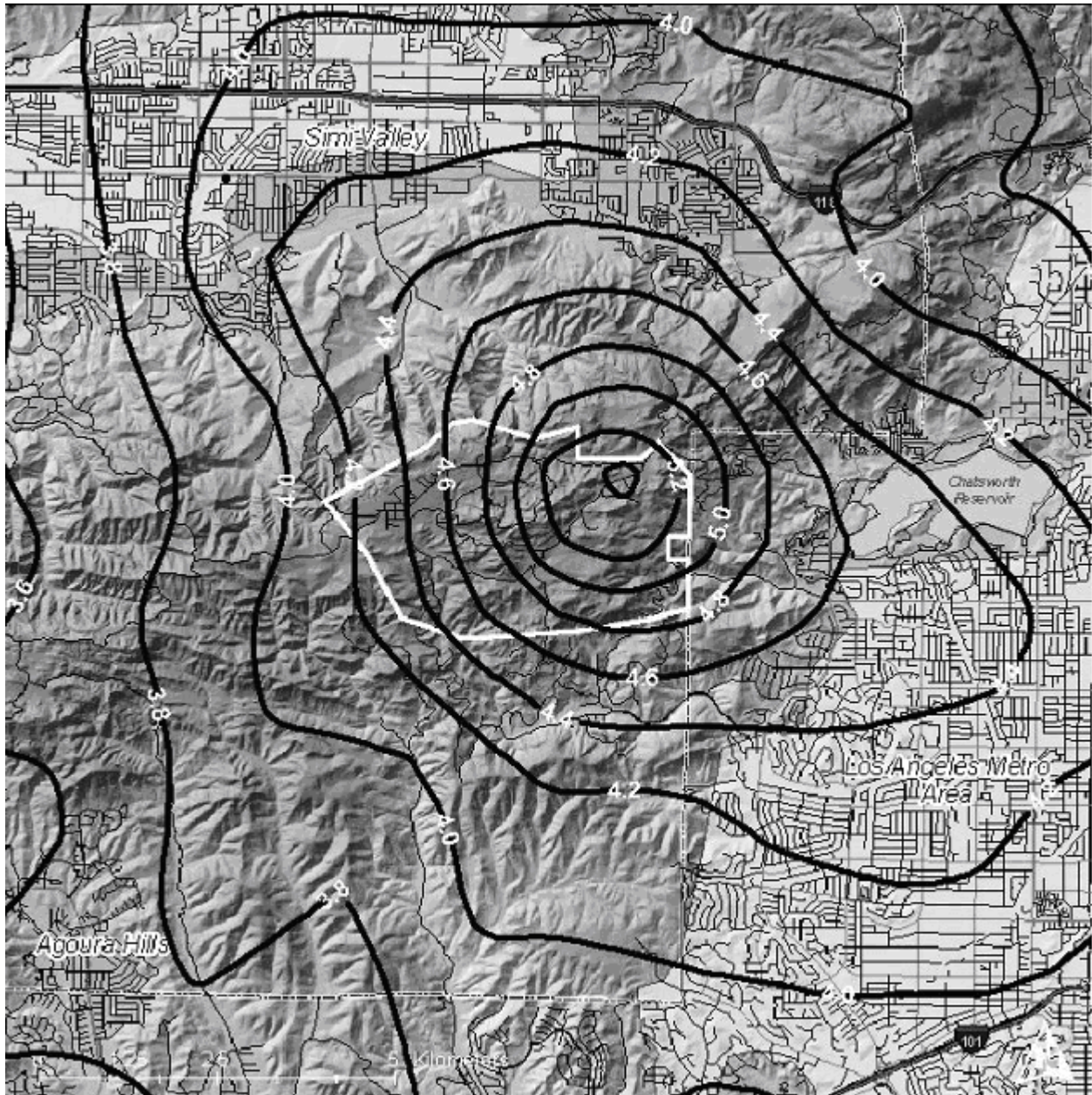


Figure 3-15. Change in the Peak Hourly Concentrations Downwind of the SSFL Property Boundary

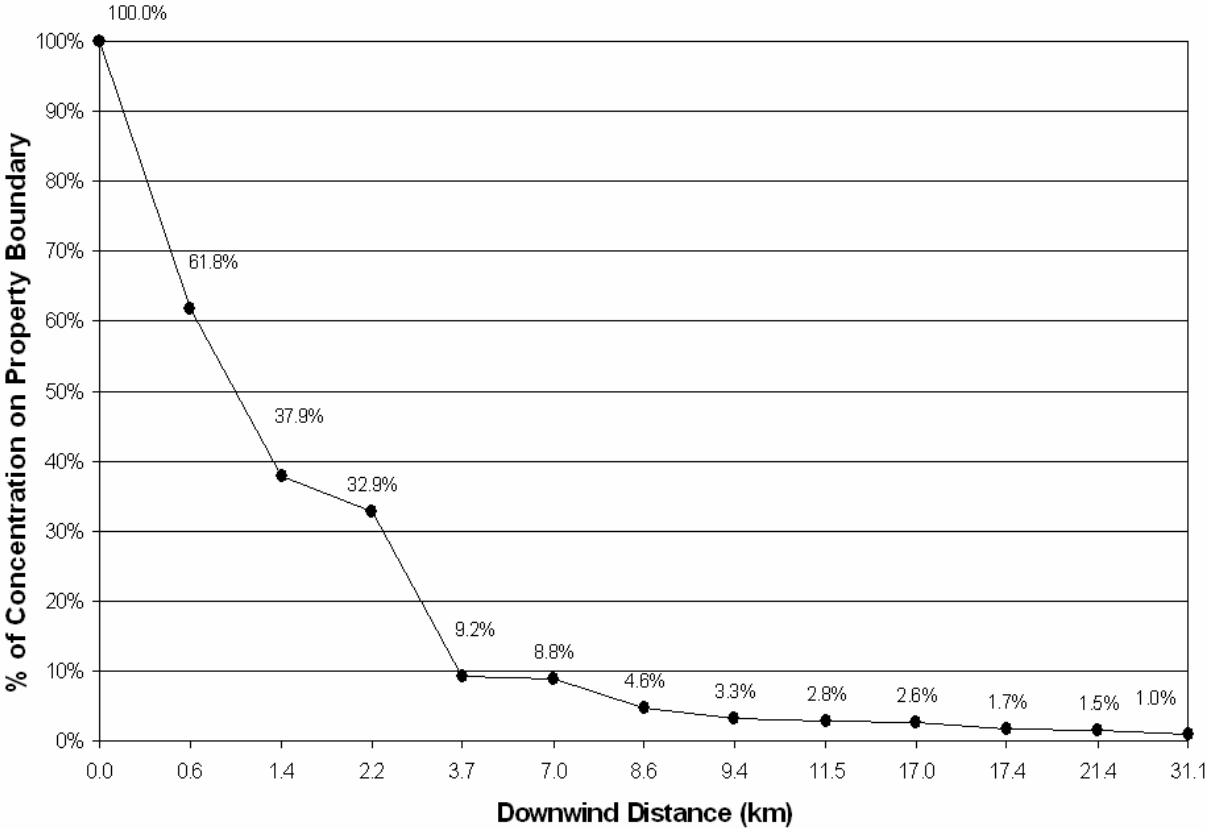


Figure 3-16. Average Concentration Pattern for all ST Point Sources Using the Best-Estimate Uniform Diurnal Emissions Profile

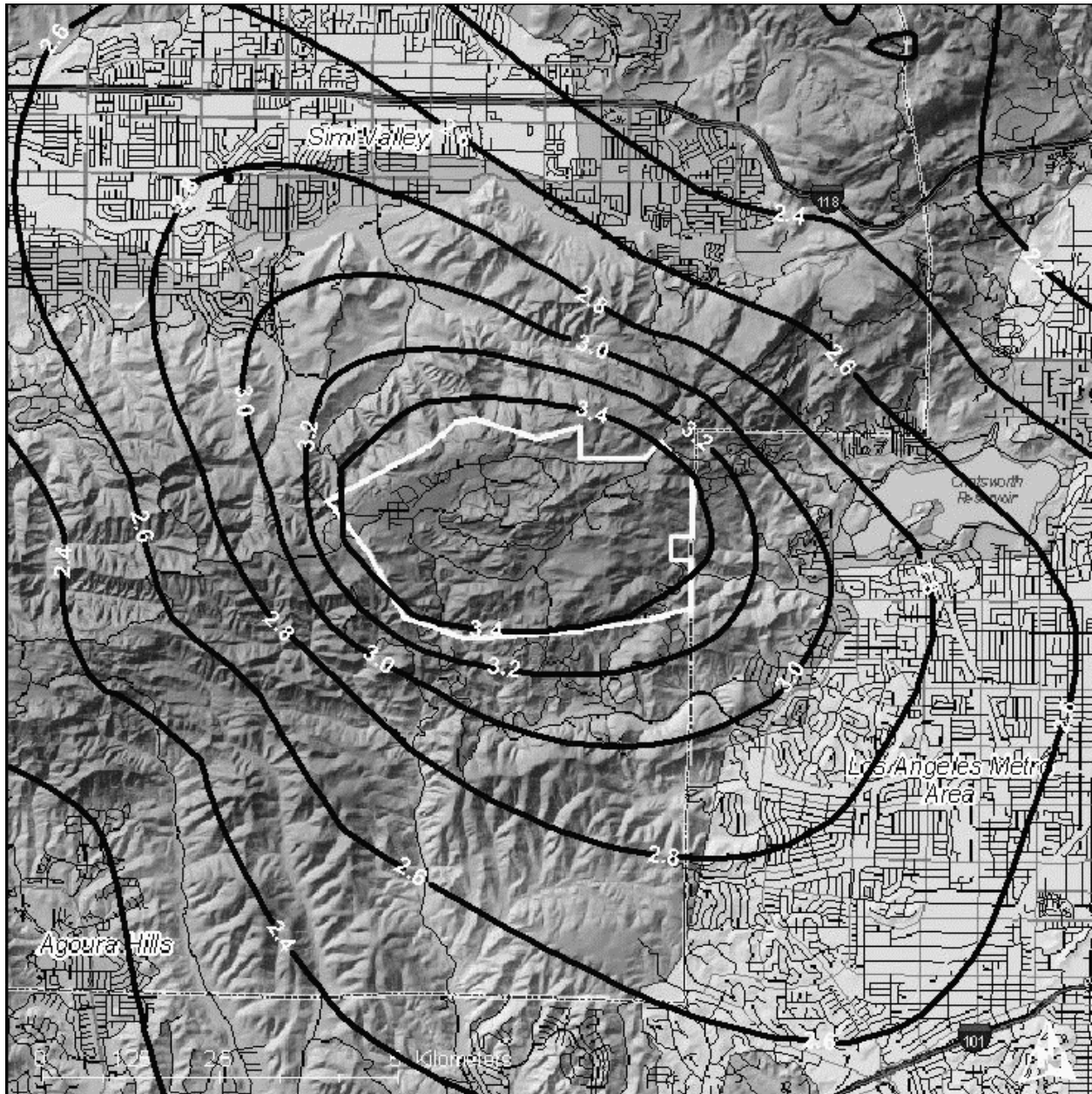


Figure 3-17. Average Concentration Pattern for all TTF Point Sources Using the Best-Estimate (Daylight Only) Diurnal Emissions Profile



3.3.5 SSFL Concentration Profiles from Air Dispersion Modeling of Emissions

It is instructive to display the chemical concentrations profile on a linear trajectory from the source to the receptor of interest. Such a concentration profile displays the concentration decay as one moves away from SSFL. Accordingly, a series of concentration profiles were calculated based on the concentration fields obtained for the different source emission scenarios (TCE/rocket engine degreasing; TCE/storage tank releases and stripping towers; and hydrazine and derivatives/open-pit burning). For each scenario, concentration-distance profiles are presented for the northwest, northeast, and southeast directions, which cover the nearest populated areas and the zones with the expected highest concentrations.

Four different profiles were determined for each of the above cases (Figures 3-18 through 3-29). The first profile is for the annually averaged concentrations, based on the air dispersion simulations for the estimated maximum annual emission rate as given in Appendix S. The second profile is for the annually averaged concentrations, based on the air dispersion simulations for the average annual emission for the 1995–1990 period for TCE and the 1959–1989 period for hydrazine. The third profile depicts the peak hourly concentration decay, based on dispersion simulations for the estimated maximum annual emission rate. Finally, the fourth profile is for the peak hourly concentration based on the dispersion simulations for the average annual emission. In the present analysis, concentration profiles were calculated based on the average concentrations for each type of emitter (e.g., the average of the eight RET stands). Note that for a given point source and climatic conditions, the concentration, at a given receptor location, is directly proportional to the emission rate. Therefore, it is convenient to present the annually averaged concentration profiles as derived from air dispersion simulations for average and maximum emission rates on the same figures. These two profiles will coincide when they are depicted in the same figure with different but properly scaled coordinate axes (Figures 3-18, 3-20, 3-22, 3-24, 3-26, and 3-28). Similarly, the peak hourly concentration profiles (Figures 3-19, 3-21, 3-23, 3-25, 3-27, and 3-29), for both average and maximum emission rates, for each chemical activity and direction, are plotted with the coordinate axes scaled so that profiles are coincident.

3.3.5.1 TCE Concentration Profiles Associated with Rocket Engine Degreasing

The averaged annual TCE concentration profiles in the northwest, northeast, and southeast directions are provided in Figures 3-18 through 3-20. The concentration on the left axis corresponds to the average during 1959, when the estimated emission rate was at maximum (~387 tons/year), while the right ordinate axis corresponds to the average concentration corresponding to the simulations at the average emission (~89 tons/year) for 1955 through 1990. For the year of maximum emission rate, the average annual concentration decreased from 17.2 $\mu\text{g}/\text{m}^3$ at the source to 1 $\mu\text{g}/\text{m}^3$ at a distance of 2.4 kilometers northwest of SSFL (Figure 3-18) and a distance of 2.0 kilometers northeast (Figure 3-20). In the southeast, the concentration decay is less pronounced, with the concentration slightly above 1 $\mu\text{g}/\text{m}^3$ even at the distance of 10.6 km away from SSFL (Figure 3-22).

The peak hourly concentration profiles in the northwest, northeast, and southeast directions are shown in Figures 3-19, 3-21, and 3-23, respectively, for the maximum emission rate (387 tons per year) and the average emission rate (~90 tons per year). These variations in the peak concentrations with distance are less sensitive to the different directions than the annual average concentrations. The profile along the northeast direction (Figure 3-21) shows a local maximum approximately 8 kilometers from the emission point, where the region topology induces a significant concentration pattern variation—as shown in the contour plot, Figure 4-8, of the *Dispersion* report of Sonoma (Appendix I). This apparent local maximum anomaly is also shown in Figure 3-27 for the TCE emissions from storage tanks and stripping towers.

3.3.5.2 TCE Concentration Profiles Associated with Storage Tank Releases and Stripping Towers

The average annual concentrations in the northwest, northeast, and southeast directions, for the maximum and average emission rates, are depicted in Figures 3-24, 3-26, and 3-28, respectively. For the maximum emission rate, the concentration decreases from the maximum value of about $20 \mu\text{g}/\text{m}^3$ at the source to $1 \mu\text{g}/\text{m}^3$ approximately 2 kilometers away from SSFL for all the three directions, as can also be seen in Figure 3-16. The weak direction-dependence of the concentration decay is also observed in Figure 3-12. The corresponding peak hourly concentrations are shown in Figures 3-25, 3-27, and 3-29.

3.3.5.3 Hydrazine and Derivatives Concentration Profiles Associated with Open-Pit Burning

The annual average concentration-distance profiles for hydrazine, based on a uniform daytime emission rate from the TTF (Section S) are provided in Figures 3-30, 3-32, and 3-34. Note that a more gradual concentration decline is observed in the southeast, relative to the northeast and northwest, as can also be seen in the concentration contour plots shown in Figure 3-17. The concentration declines from about $0.039 \mu\text{g}/\text{m}^3$ at SSFL to about $5 \times 10^{-3} \mu\text{g}/\text{m}^3$ 2 kilometers to the northwest; the same concentration decline is observed 1.4 kilometers northeast and 3.6 kilometers southeast. The peak hourly concentration profiles, Figures 3-31, 3-33, and 3-35, all show similar concentration decline profiles irrespective of direction.

Figure 3-18. Average TCE Concentration Associated with Rocket Engine Degreasing. Profile from SSFL to UTM coordinates (338, 3796) for the estimated maximum annual emission (387 tons/year) and for the estimated average emission from 1955 to 1990 (88.7 tons/year).

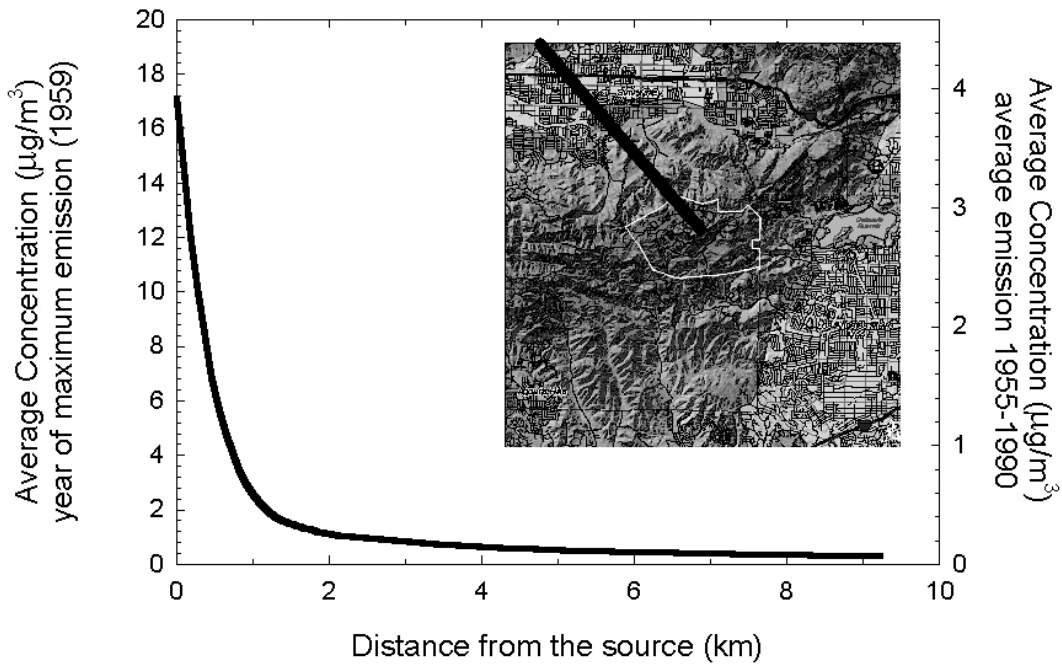


Figure 3-19. Peak Hourly TCE Concentration Associated with Rocket Engine Degreasing. Profile from SSFL to UTM coordinates (338, 3796) for the estimated maximum annual emission (387 tons/year) and for the estimated average emission from 1955 to 1990 (88.7 tons/year).

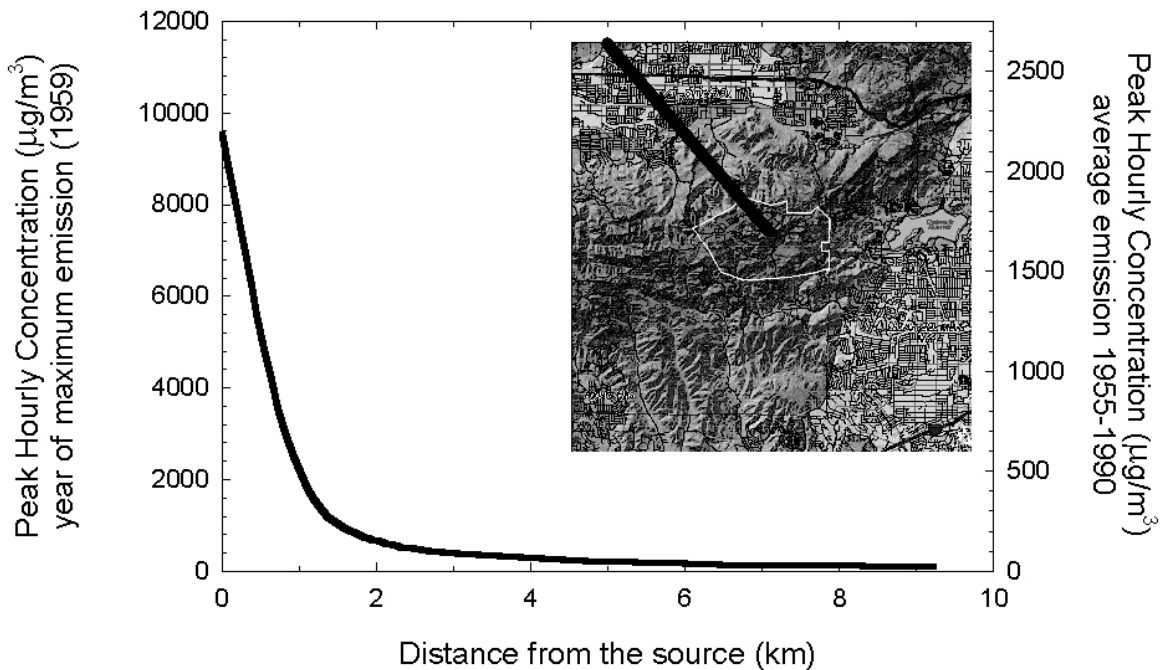


Figure 3-20. Average TCE Concentration Associated with Rocket Engine Degreasing. Profile from SSFL to UTM coordinates (351, 3796) for the estimated maximum annual emission (387 tons/year) and for the estimated average emission from 1955 to 1990 (88.7 tons/year).

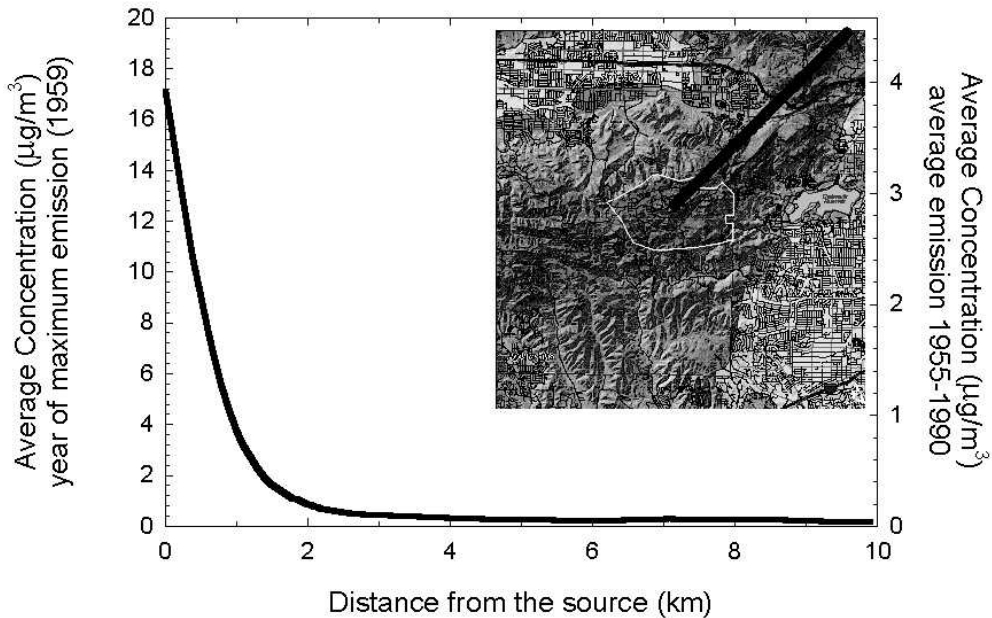


Figure 3-21. Peak Hourly TCE Concentration Associated with Rocket Engine Degreasing. Profile from SSFL to UTM coordinates (351, 3796) for the estimated maximum annual emission (387 tons/year) and for the estimated average emission from 1955 to 1990 (88.7 tons/year).

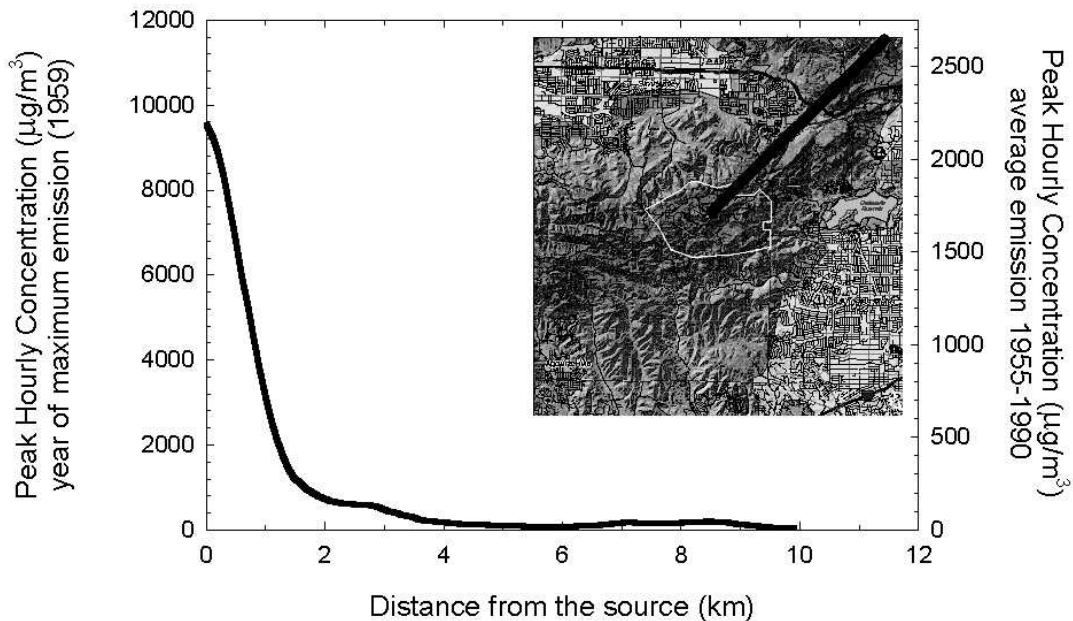


Figure 3-22. Average TCE Concentration Associated with Rocket Engine Degreasing. Profile from SSFL to UTM coordinates (351, 3781) for the estimated maximum annual emission (387 tons/year) and for the estimated average emission from 1955 to 1990 (88.7 tons/year).

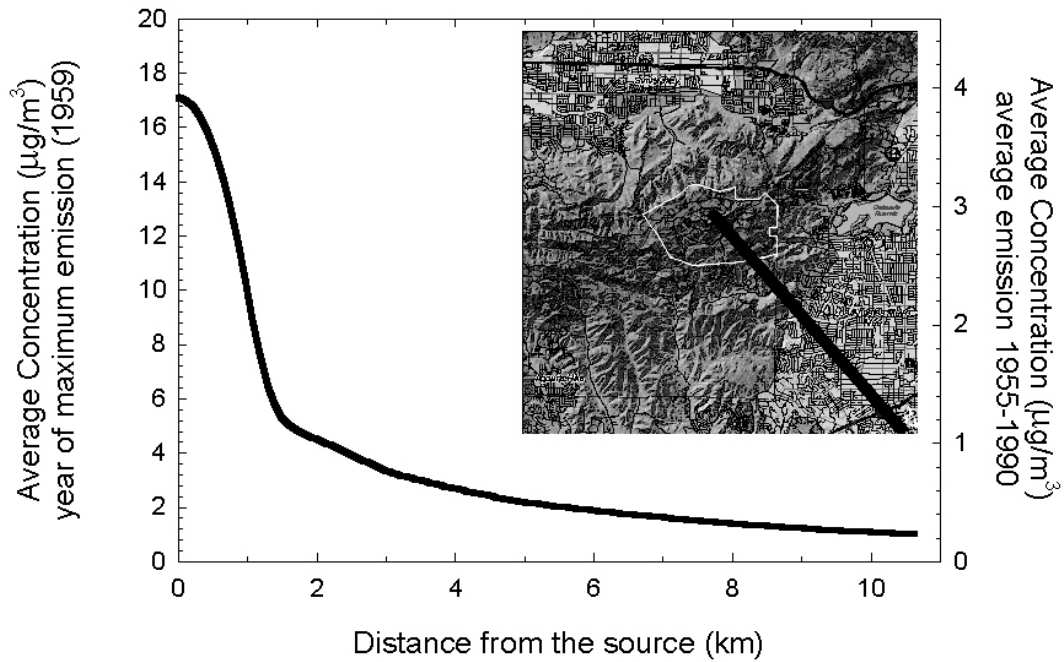


Figure 3-23. Peak Hourly TCE Concentration Associated with Rocket Engine Degreasing. Profile from SSFL to UTM coordinates (351, 3781) for the estimated maximum annual emission (387 tons/year) and for the estimated average emission from 1955 to 1990 (88.7 tons/year).

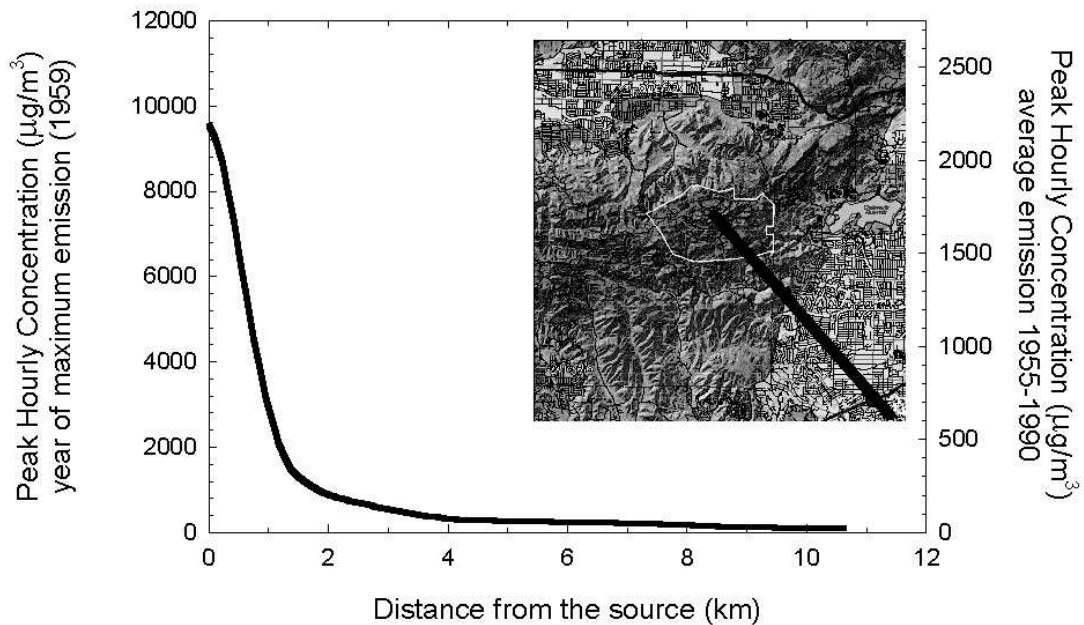


Figure 3-24. Average TCE Concentration Associated with Storage Tank Releases and Stripping Towers. Profile from SSFL to UTM coordinates (338, 3796) for the estimated maximum annual emission (91.8 tons/year) and for the estimated average emission from 1955 to 1990 (21.8 tons/year).

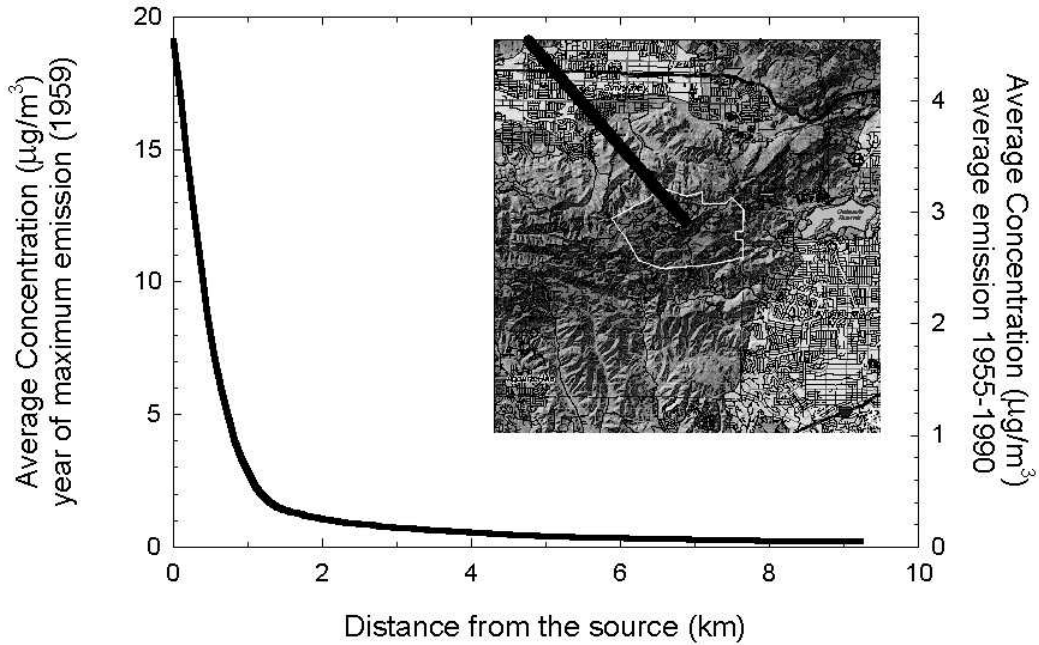


Figure 3-25. Peak Hourly TCE Concentration Associated with Storage Tank Releases and Stripping Towers. Profile from SSFL to UTM coordinates (338, 3796) for the estimated maximum annual emission (91.8 tons/year) and for the estimated average emission from 1955 to 1990 (21.8 tons/year).

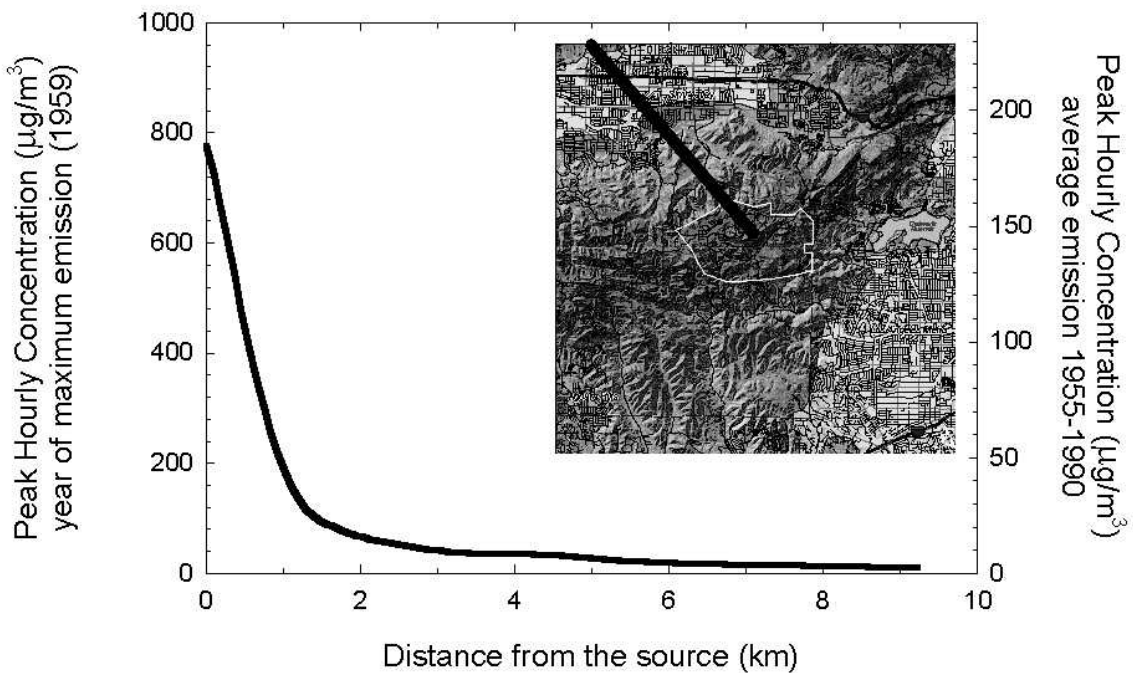


Figure 3-26. Average TCE Concentration Associated with Storage Tank Releases and Stripping Towers. Profile from SSFL to UTM coordinates (351, 3796) for the estimated maximum annual emission (91.8 tons/year) and for the estimated average emission from 1955 to 1990 (21.8 tons/year).

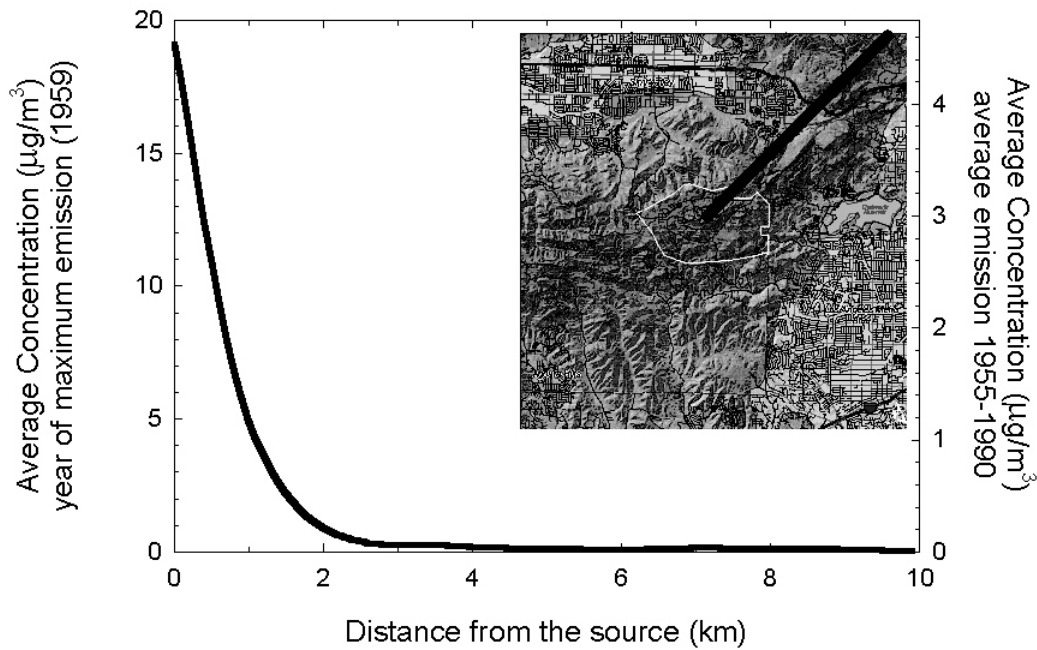


Figure 3-27. Peak Hourly TCE Concentration Associated with Storage Tank Releases and Stripping Towers. Profile from SSFL to UTM coordinates (351, 3796) for the estimated maximum annual emission (91.8 tons/year) and for the estimated average emission from 1955 to 1990 (21.8 tons/year).

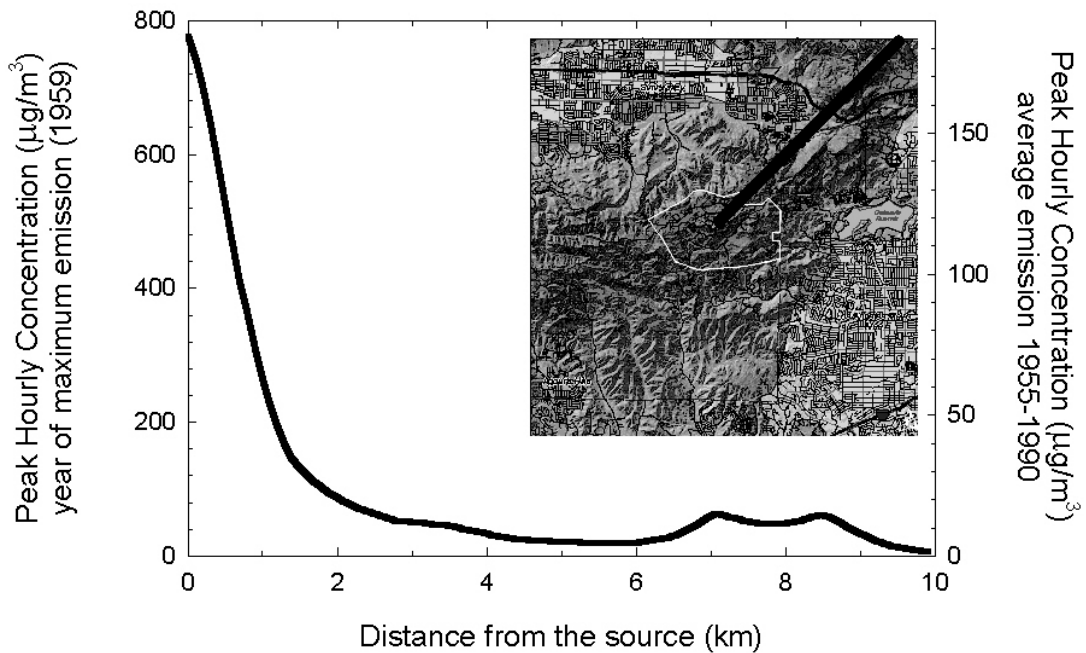


Figure 3-28. Average TCE Concentration Associated with Storage Tank Releases and Stripping Towers. Profile from SSFL to UTM coordinates (351, 3781) for the estimated maximum annual emission (91.8 tons/year) and for the estimated average emission from 1955 to 1990 (21.8 tons/year).

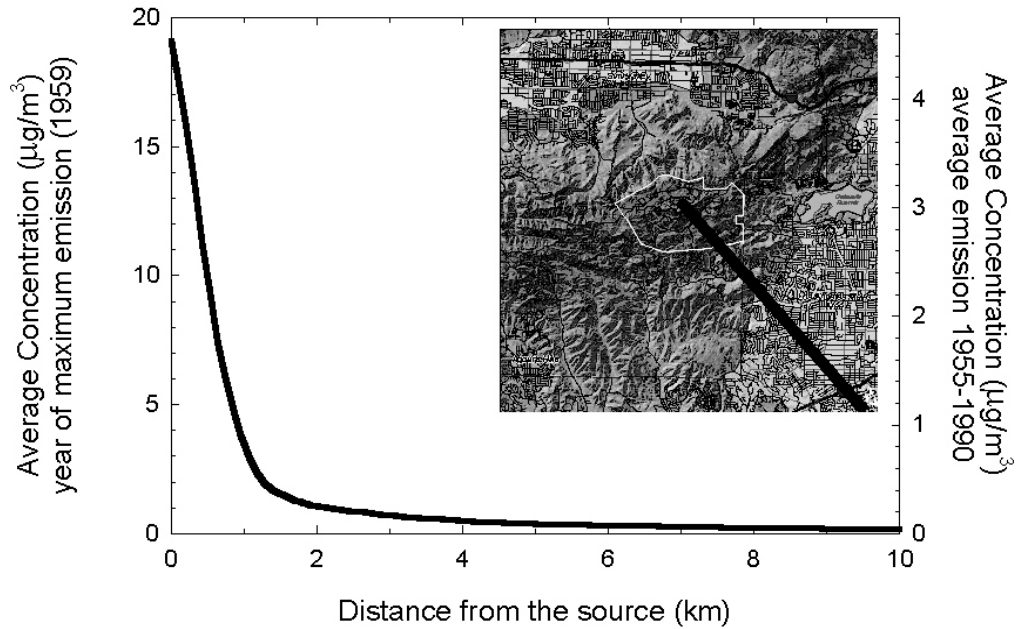


Figure 3-29. Peak Hourly TCE Concentration Associated with Storage Tank Releases and Stripping Towers. Profile from SSFL to UTM coordinates (351, 3781) for the estimated maximum annual emission (91.8 tons/year) and for the estimated average emission from 1955 to 1990 (21.8 tons/year).

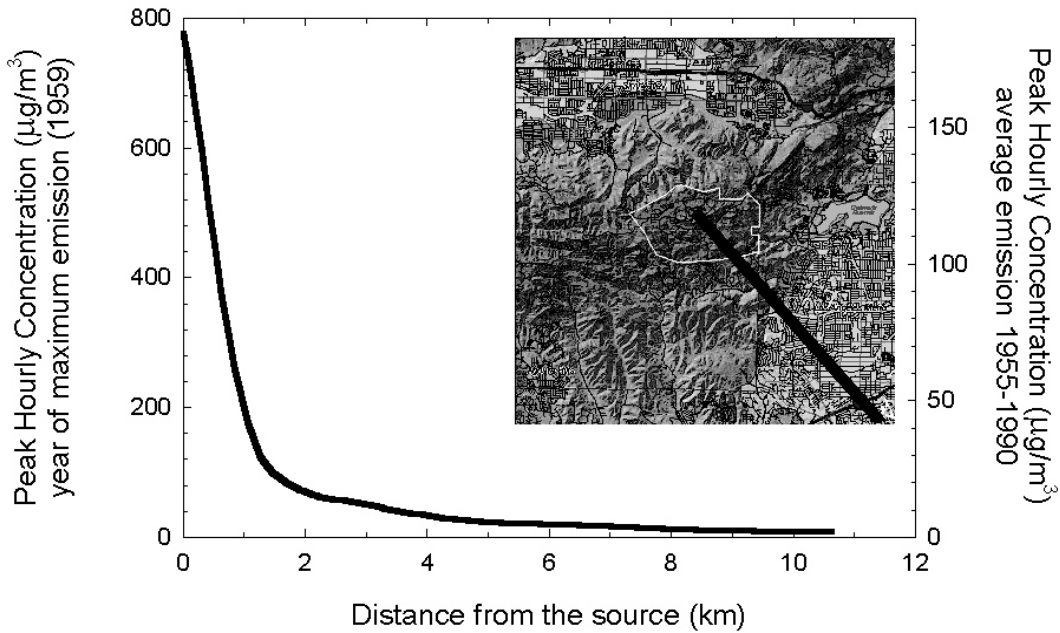


Figure 3-30. Average Hydrazine and Derivatives Concentration Associated with Open-Pit Burning. Profile from SSFL to UTM coordinates (338, 3796) for the estimated uniform emission (0.658 tons/year).

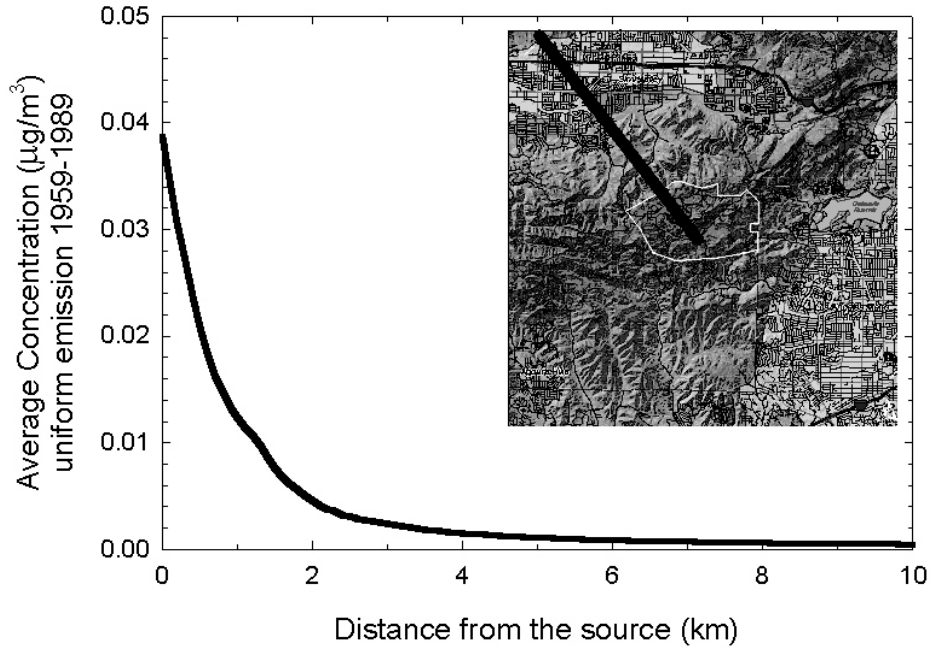


Figure 3-31. Peak Hourly Hydrazine and Derivatives Concentration Associated with Open-Pit Burning. Profile from SSFL to UTM coordinates (338, 3796) for the estimated uniform emission (0.658 tons/year).

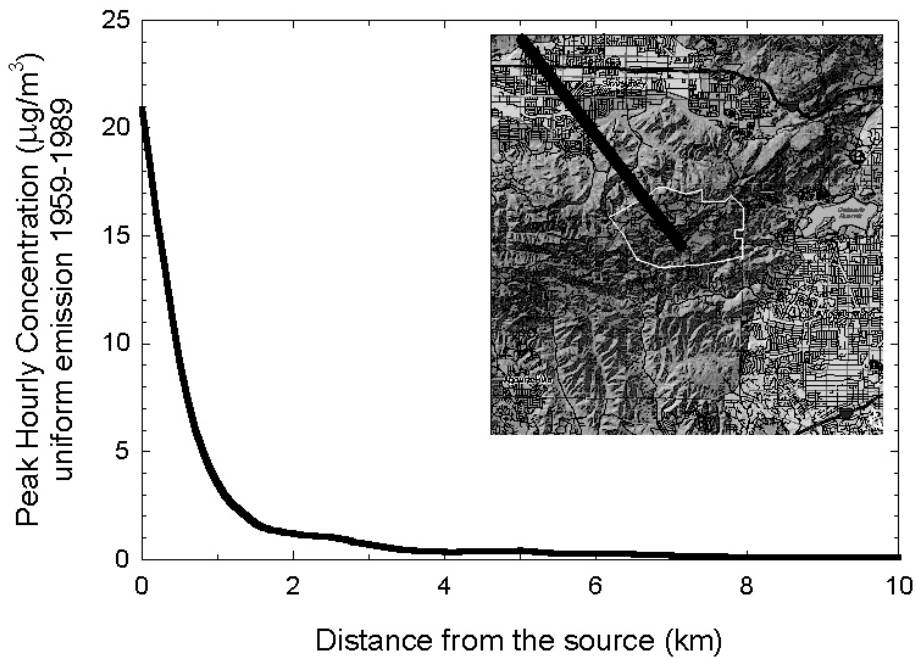


Figure 3-32. Average Hydrazine and Derivatives Concentration Associated with Open-Pit Burning. Profile from SSFL to UTM coordinates (351, 3796) for the estimated uniform emission (0.658 tons/year).

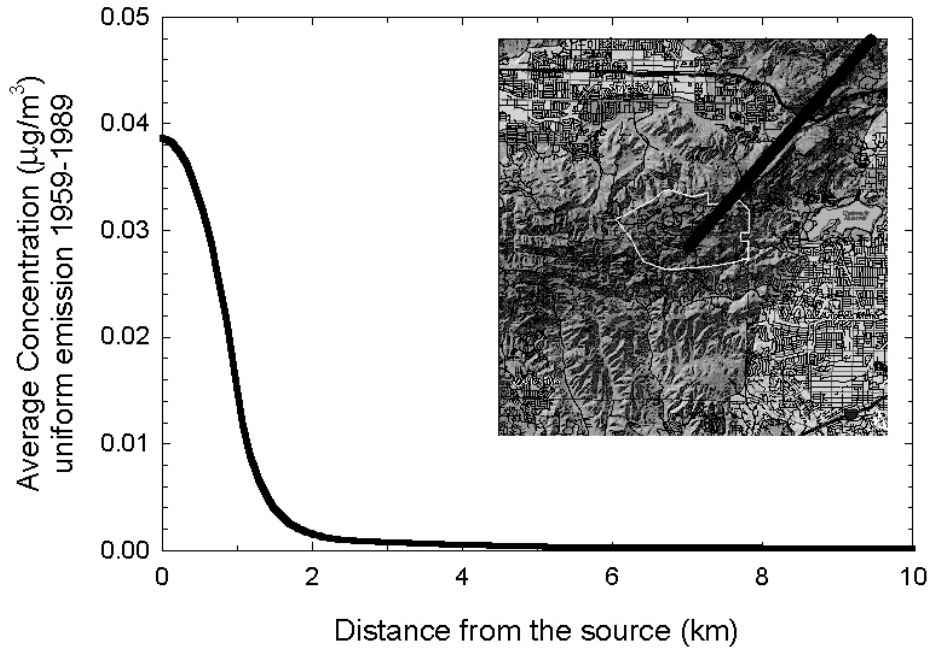


Figure 3-33. Peak Hourly Hydrazine and Derivatives Concentration Associated with Open-Pit Burning. Profile from SSFL to UTM coordinates (351, 3796) for the estimated uniform emission (0.658 tons/year).

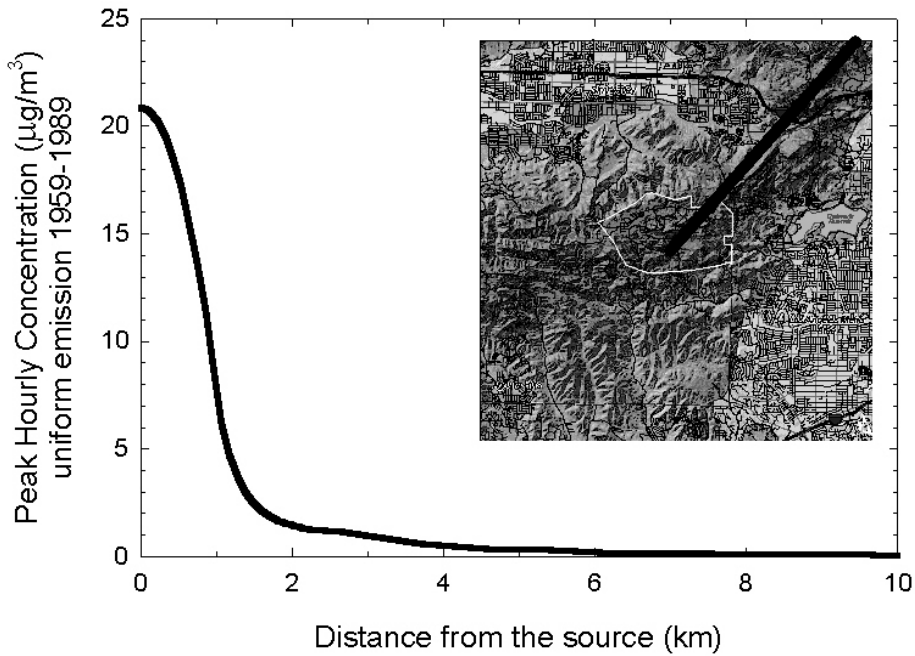


Figure 3-34. Average Hydrazine and Derivatives Concentration Associated with Open-Pit Burning. Profile from SSFL to UTM coordinates (351, 3781) for the estimated uniform emission (0.658 tons/year).

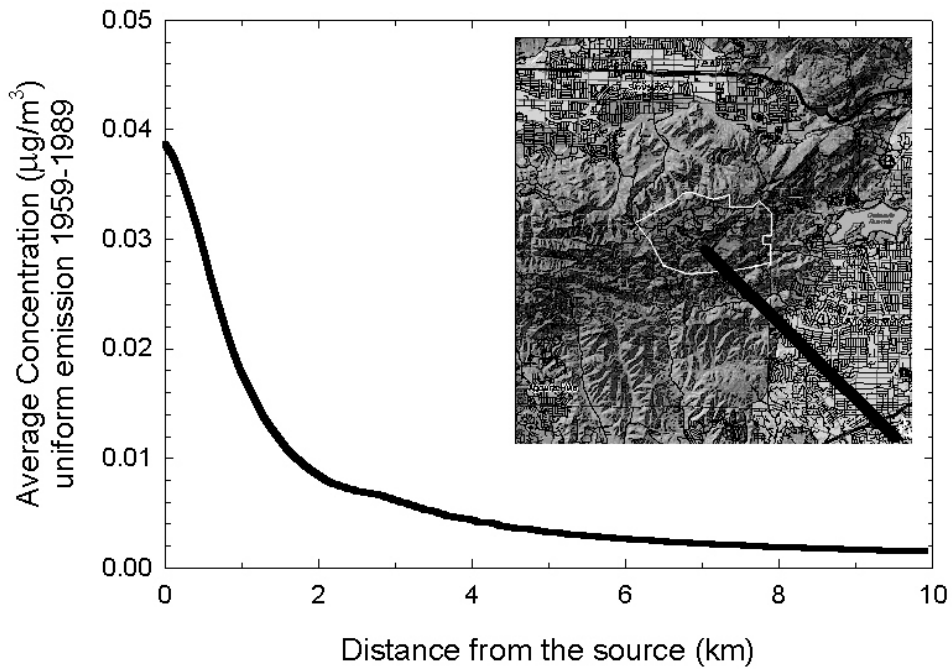
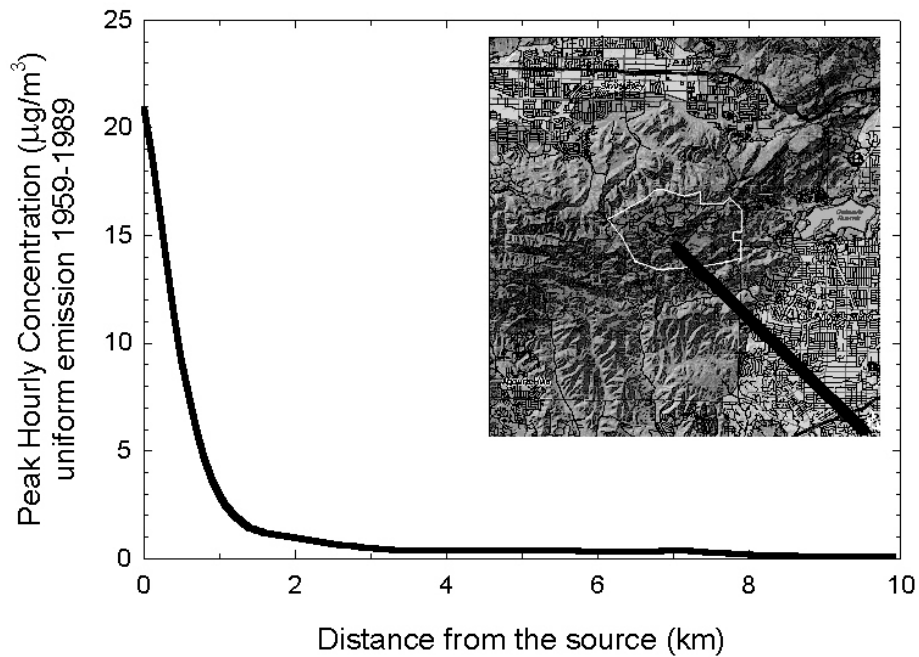


Figure 3-35. Peak Hourly Hydrazine and Derivatives Concentration Associated with Open-Pit Burning. Profile from SSFL to UTM coordinates (351, 3781) for the estimated uniform emission (0.658 tons/year).



3.3.6 Sensitivity Studies

The estimated airborne concentrations of SSFL emitted chemicals in populated areas surrounding SSFL were calculated following U.S. Environmental Protection Agency (USEPA) modeling guidance^{3.3}. In this approach all four-years of Area IV on-site meteorological data were utilized to estimate hourly average atmospheric concentrations of air toxics associated with SSFL emissions. Long-term averages were also obtained in addition to 1-hour and 24-hour maximum concentrations. The estimated air toxic concentrations did not consider atmospheric chemical degradations, dry deposition and rain scavenging. The above simplification was justified given the following argument. The reaction half-life for most organics is longer than their time of travel from SSFL across the study area. The rate of dry deposition of particle-bound chemicals is sufficiently slow and thus the impact on estimated concentrations within the study area would be small. Moreover, the particle size distributions from rocket engine tests are not known and thus could not be accurately incorporated into the model simulations. Wet deposition is episodic and given the low annual rainfall, rain scavenging of chemicals would have a negligible effect on the annual average long-term concentrations. It is emphasized that the consequence of neglecting atmospheric degradation and dry and wet deposition is a conservative (i.e., overestimate) estimate of atmospheric concentrations of SSFL emitter chemicals. A detailed discussion of the sensitivity studies conducted to assess the impact of the above model simplifications is provided in Appendix I.

While the various simulations discussed in Chapter 3 focus on annual averaged concentrations, these estimates do not identify the extent of potential exposure to significantly higher or lower concentrations in a single year. In order to identify the specific periods and level of highest exposure concentrations, there is need for accurate data regarding the number and timing of rocket tests and the meteorology associated with those tests. Unfortunately, the meteorology associated with individual tests may be difficult to reconstruct lacking routine nearby meteorological measurements from the start of testing (1948) to present (2004). The highest exposure concentrations for the population surrounding SSFL would be at the SSFL boundary. As suggested by the sensitivity studies (Appendix I), concentrations at the SSFL boundary could be up to a few orders of magnitude higher than the average airborne air toxic concentrations to which the population surrounding SSFL was exposed.

^{3.3} Appendix W of 40 CFR 51.